Check for updates

Received: 22 August 2022 | Revised: 24 October 2022 | Accepted: 25 October 2022

DOI: 10.1002/ptr.7670

RESEARCH ARTICLE

WILEY

Antcin A, a phytosterol regulates SARS-CoV-2 spike protein-mediated metabolic alteration in THP-1 cells explored by the ^{1}H-NMR-based metabolomics approach

Gyaltsen Dakpa[1,2] | Kanthasamy Jayabal Senthil Kumar[3] | Nai-Wen Tsao[4] | Sheng-Yang Wang[1,3,4,5]

[1]Molecular and Biological Agricultural Sciences Program, Taiwan International Graduate Program, Academia Sinica, Taipei, Taiwan

[2]Graduate Institute of Biotechnology, National Chung-Hsing University, Taichung, Taiwan

[3]Bachelor Program of Biotechnology, National Chung Hsing University, Taichung, Taiwan

[4]Department of Forestry, National Chung-Hsing University, Taichung, Taiwan

[5]Agricultural Biotechnology Research Center, Academia Sinica, Taipei, Taiwan

Correspondence
Sheng-Yang Wang, Department of Forestry, National Chung-Hsing University, 250 Kuo-Kuang Road, Taichung, 402, Taiwan.
Email: taiwanfir@dragon.nchu.edu.tw

Abstract

The mechanism of SARS-CoV-2 spike protein-mediated perturbations of metabolic pathways and modulation of antcin A, a steroid-like compound isolated from *Taiwanofungus camphoratus*, are not studied. Here, we investigated the metabolic alteration by SARS-CoV-2 spike protein and the regulatory effect of antcin A on SARS-CoV-2 spike protein-induced metabolic changes in the Phorbol 12-myristate 13-acetate (PMA)-induced human monocytes (THP-1) using proton nuclear magnetic resonance (^{1}H-NMR) and MetaboAnalyst 5.0 software. The cytotoxic potential of SARS-CoV-2 spike protein, antcin A, and dexamethasone was assessed by MTT assay. The metabolomic perturbations and their relation to human coronaviruses' receptors were evaluated by qPCR. This study indicated that the altered metabolites mediated by SARS-CoV-2 protein, such as methionine, phosphoenolpyruvic acid, canadine, glutamine, ethanolamine, and phenylalanine, were significantly reversed by antcin A. In addition, antcin A significantly inhibited SARS-CoV-2 spike protein-mediated up-regulation of TLR-4 and ACE2 receptors, while GRP78 inhibition was not statistically significant. This is the first study to use ^{1}H-NMR to investigate SARS-CoV-2 spike protein-induced metabolomic changes in PMA-induced THP-1 cells. Antcin A significantly reversed metabolomic alters while dexamethasone failed to fix them. Therefore, we believe that antcin A could be a potential candidate for therapeutic agents for viral infections related to a metabolic abnormality.

KEYWORDS

^{1}H-NMR, antcin A, metabolomics, SARS-CoV-2 spike protein, *Taiwanofungus camphoratus*

1 | INTRODUCTION

The coronavirus disease-2019 (COVID-19) is one of the top 20 worst pandemics in world history (Feehan & Apostolopoulos, 2021), which is caused by severe acute respiratory syndrome coronavirus 2 (SARS-CoV-2), which is approximately 50–200 nm in diameter with lipid enveloped and has single-stranded ribonucleic acid (+ss-RNA) genomes of 30 kb. It consists of the viral open reading frames (ORFs) encoding structural, non-structural, and accessory proteins. Non-structural and additional proteins participate in viral replication or modify polymerase fidelity or modulation of nucleotide incorporation. The spike (S), membrane (M), envelope (E), and nucleocapsid (N) are structural proteins (Lu et al., 2020; Malone, Urakova, Snijder, & Campbell, 2022) for their vital role in the life cycle of the viral particles. Among the structural proteins, the spike protein is responsible for binding to receptors and facilitating membrane fusion in the host cells, contributing to the severity of the COVID-19 (Wrapp et al., 2020). SARS-CoV-2 spike uses the angiotensin-converting enzyme

 © 2022 John Wiley & Sons Ltd.

10991573, 0, Downloaded from https://onlinelibrary.wiley.com/doi/10.1002/ptr.7670 by Natl Chung Hsing University, Wiley Online Library on [22/11/2022]. See the Terms and Conditions (https://onlinelibrary.wiley.com/terms-and-conditions) on Wiley Online Library for rules of use; OA articles are governed by the applicable Creative Commons License

2 (ACE2) as a receptor to enter and fusion the cells (Shang et al., 2020), which also triggers the severity of COVID-19. The seriousness of COVID-19 is not solely relying on the binding of SARS-CoV-2 on ACE2. Moreover, it activates the pathogen recognition receptors (PPRs) like Toll-like receptor-4 (TLR-4) to induce a hyper-inflammation (Zhao et al., 2021). Glucose-regulated protein (GRP-78) has another receptor-binding domain (RBD) binding site of SARS-CoV-2. Putative interaction between GRP78 and the RBD of the SARS-CoV-2 spike protein causes inflammation. This was further confirmed by an in vitro study in which GRP-78 directly binds to ACE2 of the RBD of the spike. Knocking out GRP-78 reduces the surface expression of ACE2 in the VeroE6 (Carlos et al., 2021; Nassar et al., 2021), which induces hyperinflammation. Thus, the activation of viral receptors like GRP-78, TLR4, and ACE2 is one of the primary causes of death in COVID-19 patients (Merad & Martin, 2020) by inducing hyper-inflammation is well established. On the other hand, several studies have revealed that the severity and progress of COVID-19 are associated with the metabolomic alteration (Wu et al., 2020). Plasma metabolic abnormalities, including a shift toward amino acid and fatty acid synthesis, altered energy, and lipid metabolism, are also categorized as landmarks of the COVID-19-related death (Thomas et al., 2020). However, the mechanism by which SARS-CoV-2 spike protein perturbs metabolic pathways is unclear.

Taiwanofungus camphoratus (syn. *Antrodia cinnamomea*, *Antrodia camphorata*) belongs to the class Agaricomycetes and order Polyporales and is an edible medicinal fungus native to Taiwan. It grows only in the inner cavity of the endemic species *Cinnamomum kanehirae* Hayata (Lauraceae) (Chen et al., 2011). The host plant is a large evergreen broad-leaved tree distributed over broad-leaved forests at an altitude of 200–2000 m. It grows in most mountains in Taiwan, like Taoyuan, Miaoli, Nantou, Kaohsiung, Taitung, and Hualien of Taiwan (Geethangili & Tzeng, 2011). The fruiting bodies of *T. camphoratus* were traditionally used to treat liver diseases, drug intoxication, diarrhea, abdominal pain, hypertension, and tumorigenic diseases. More than 18 antcins were isolated from the fruiting bodies of *T. camphoratus*. Among them, antcin A, B, C, H, and K, are dominant in *T. camphoratus*. We previously reported that antcin A mimics glucocorticoids and causes transcription of the glucocorticoid receptor, suppressing inflammation in A549 lung cells. In contrast, other antcins such as antcin B, C, H, and K were failed to inhibit inflammation (Chen et al., 2011). Hence, it is reasonable to hypothesize that antcin A may inhibit human coronavirus receptors like ACE2, TLR4, and GRP-78, a mechanism by which SARS-CoV-2 induces hyperinflammation in patients with COVID-19. In addition, antcin A shares structural similarities with dexamethasone, a synthetic glucocorticoid used to treat COVID-19 (Group et al., 2020). Except antcin A, other antcins, including antcin B, K, C, and H, have OH or O functional groups at the C_7 position. Indeed, both dexamethasone and antcin A have no function group at the C_7 position; this may contribute to the antiinflammatory properties of antcin A. Nevertheless, antcin A has significant differences in other functional groups of dexamethasone, which cause differences in their activity, as shown in Figure 1. Antcins-analogs have an inhibitory effect against the p38-MAPK signaling, which is another promising strategy for treating COVID-19 (Grimes & Grimes, 2020; Senthil Kumar et al., 2020) as the other natural compound like papaverine, chelerythrine, losmapimod, and dilmapimod are reported potentially to use for the treatment of the COVID-19 via inhibitory of the p38-MAPK signaling (Valipour, Irannejad, & Emami, 2022a, 2022b; Valipour, Zarghi, Ebrahimzadeh, & Irannejad, 2021). Recently, we reported that antcin A could block ACE2 activity in HT-29 cells (Kumar, Vani, Hsieh, Lin, & Wang, 2021), which indicates that it might be a potential prophylactic agent for COVID-19. However, there is still minimal scientific evidence for the effects of antcin A on SARS-CoV-2-induced metabolic alterations in host cells. Several studies have reported that metabolomics correction is one of the suitable adjunct treatments to enhance clinical outcomes because metabolic abnormality leads to many diseases, including cancers, diabetes mellitus (DM), Alzheimer's disease,

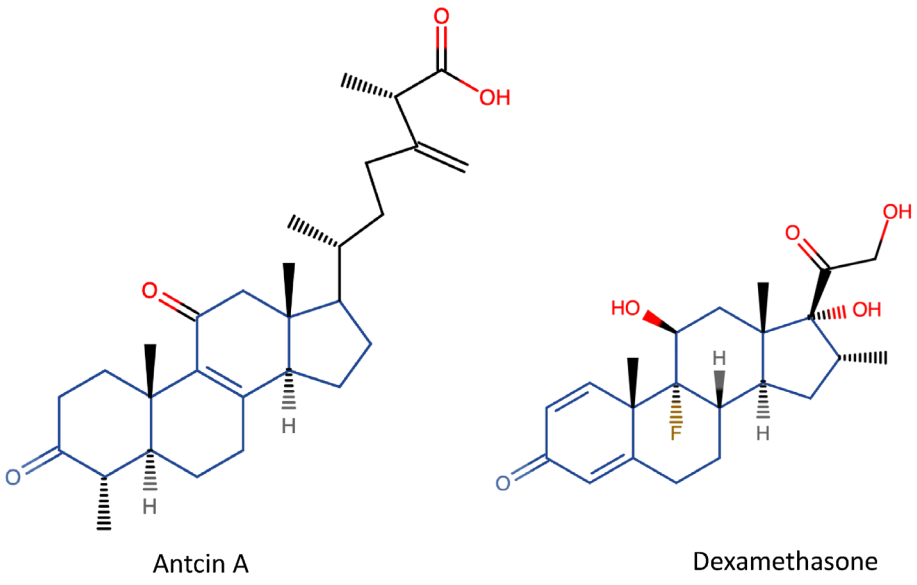

FIGURE 1 The structure of the antcin A and dexamethasone. The backbone of the antcin A and dexamethasone, represented in blue colors, are similar. The color-coded red and black is represented the function and another group of compounds that make a difference in the activities of the Antcin A from the dexamethasone.

10991573, 0, Downloaded from https://onlinelibrary.wiley.com/doi/10.1002/ptr.7670 by Natl Chung Hsing University, Wiley Online Library on [22/11/2022]. See the Terms and Conditions (https://onlinelibrary.wiley.com/terms-and-conditions) on Wiley Online Library for rules of use; OA articles are governed by the applicable Creative Commons License

cardiovascular diseases (CVDs), and liver cirrhosis (Miranda-Massari et al., 2016; Wishart, 2019).

Various experimental studies can elucidate cellular metabolic alterations, including metabolomic methods, molecular-level investigation, and integrative analysis of "omic" data involving proteomics and genomics-scale study (Abdul-Hamid et al., 2019). A comprehensive analysis of cellular metabolism may provide insight into biological systems. Cell metabolomics has recently been recognized as essential for determining cellular metabolite profiles and characterizing perturbed metabolic pathways. These metabolites are generally the ultimate downstream products of gene transcription; hence, their modification is anticipated to be intensified. Meanwhile, identifying metabolic correction may be a potential indicator of the enzymatic activities, which reflect the mechanism of action for any antiinflammatory agent. Therefore, this study aimed to investigate the metabolic alteration caused by SARS-CoV-2 spike protein on the PMA-induced THP-1 cells and investigate the regulatory effect of antcin A on SARS-CoV-2-induced metabolic changes in the host cells. ^{1}H-NMR-based metabolomics analysis was applied herein for the first time to explore the intracellular metabolite profile of PMA-induced THP-1 cells with treatment of SARS-CoV-2 spike protein and showed metabolic correction by antcin A. Additionally, altered metabolic pathways may be used to identify prominent metabolites associated with inflammation. These attempts are performed better to understand SARS-CoV-2 spike protein-mediated metabolic alteration and their consequences and develop therapeutic strategies for COVID-19.

2 | MATERIALS AND METHODS

2.1 | Chemicals

Methanol-d4 (>99.8 atom% D) that contains trimethylsilyl propionic acid sodium salt (TSP) and analytical grade methanol (MeOH) for liquid chromatography was purchased from Sigma-Aldrich (St. Louis, MO, USA) and Merck (Darmstadt, Germany), respectively. High glucose Rosewell Park Memorial Institute medium 1640 (RPMI-1640), fetal bovine serum (FBS), $_{L}$-glutamine, sodium pyruvate, and penicillin–streptomycin were obtained from Hyclone/GE Healthcare Life sciences (Logan, UT, USA). Phorbol 12-myristate 13-acetate (PMA) was purchased from Sigma-Aldrich. SARS-CoV-2 spike glycoprotein (Full-Length), His-Tag (CHO): HRP. Conjugate (the native antigen; REC31868-HRP-100) was obtained from the native antigen (Kidlington, UK). Antcin A was isolated from *T. camphoratus*, as described previously by Chen et al. (2011).

2.2 | Method for purification of the Antcin

Fruiting bodies of *T. camphoratus* were obtained from the R&D Center of Taiwan Leader Biotechnology Corp. (Taichung, Taiwan). The oven-dried fruiting bodies of *T. camphoratus* (50 g) were extracted with methanol (3 × 2 L) at room temperature (7 d each). The combined extract was evaporated under reduced pressure to afford a brown residue, suspended in H_2O (1 L), and then extracted sequentially with EtOAc and n-BuOH (3 × 1 L). The EtOAc fraction (10.8 g) was subjected to silica gel chromatography (60 × 3.5 cm) using a stepwise gradient mixture of n-hexane and EtOAc as eluent. Fraction 5 was purified through a silica gel column (2 × 45 cm) and eluted with CH_2Cl_2–EtOAc (30:1 to 0:1) to obtain six fractions (each about 300 ml), 5A–F. Fraction 5C was applied to semipreparative HPLC eluted with CH_2Cl_2-acetone (40:1) to yield antcin A (5.1 mg). Fraction 6 was further chromatographed on a silica gel column (2 × 45 cm), eluted with CH_2Cl_2–EtOAc (15:1 to 0:1) to resolve into five fractions (each about 350 ml), 6A–E. Fraction 6B was subjected to semipreparative HPLC eluted with CH_2Cl_2-acetone (20:1) to yield antcin B (9.5 mg). Fraction 6C was also subjected to semipreparative HPLC eluted with CH_2Cl_2-acetone (15:1) to yield antcin C (4.5 mg). Fraction 7 was further chromatographed on a silica gel column (2 × 45 cm), eluted with CH_2Cl_2-methanol (50:1) to afford seven fractions (each about 300 ml), 7A–G. Fraction 7C was subjected to semipreparative HPLC eluted with CH_2Cl_2- acetone (9:1) to yield antcin H (6.5 mg). Fraction 9 was further purified through a silica gel column (2 × 45 cm) and eluted with CH_2Cl_2–MeOH (15:1) to obtain six fractions (each about 300 ml), 9A–F. Fraction 9 E was subjected to semipreparative HPLC eluted with CH_2Cl_2–Isopropanol (9:1) to yield antcin K (4.1 mg). The five purified antcins in a mixture of two epimers at C-25 were confirmed by their ^{1}H-NMR, ^{13}C-NMR, and HR-EI-MSN spectra (Chen et al., 2011). The structures of the antcins are described in Figure S1. The purity of all antcins is higher than 99% analyzed by HPLC and NMR spectrum.

2.3 | Cell culture and treatments

The human acute monocytic cell line (THP-1) was obtained from the Bioresource Collection and Research Centre (BCRC, Hsinchu, Taiwan) at 3 passages of the cell lines. THP-1 cells were cultured as a suspension in a 10 cm culture dish in RPMI-1640 supplemented with 10% FBS and 4 mM $_{L}$-glutamine. The culture was maintained to subculture under 5% CO_2 at 37°C for 3 days. Cells were seeded at a 2.5 × 10^6 cells/mL per 10 cm dish density at eight passages of the cells. Under culture conditions, cells were allowed to reach approximately 90% confluency after seeding. To differentiate THP-1 cells into macrophages, cells were seeded with 2.5 × 10^6 cells/mL in 100 ng/mL of PMA in 5% CO_2 at 37°C for 48 h (Richter, Ventz, Harms, & Hochgrafe, 2016). According to the cells' morphology and the cells' adhesive properties on the cells on the surface of the cells, this particular concentration was chosen (Figure S2). The cytotoxic effect of PMA was measured by the standard trypan blue cell counting method. The cells were seeded with a density of 2.5 × 10^6 cells/mL per 10 cm dish containing 100 ng/mL of PMA and incubated for 5% CO_2 at 37°C for 48 h. After removing the residual PMA, the treatment groups were as follows: Control; SARS-CoV-2 spike protein (100 ng/mL); dexamethasone (100 nM) (Dex); antcin A (20 μM); SARS-CoV-2-spike

10991573, 0, Downloaded from https://onlinelibrary.wiley.com/doi/10.1002/ptr.7670 by Natl Chung Hsing University, Wiley Online Library on [22/11/2022]. See the Terms and Conditions (https://onlinelibrary.wiley.com/terms-and-conditions) on Wiley Online Library for rules of use; OA articles are governed by the applicable Creative Commons License

(S) + antcin A; SARS-CoV-2 spike protein (S) + dexamethasone (dex); and these were maintained under 5% CO_2 at 37°C for 12 h.

2.4 | Cell toxicity assay

To investigate the cytotoxicity of the SARS-CoV-2 spike protein, natural compound antcin A isolated from the fruiting bodies of *T. camphoratus* and dexamethasone on THP-1 cells, PMA-induced THP-1 cells were seeded in 96-well plates with 5,000 cells per well in 200 μL of complete growth culture media, followed by incubation at 37°C (5% CO_2) for 48 h to allow cell differentiation and attachment. The cells were then treated with antcin A (10–50 μM), dexamethasone (25–400 nM), and SARS-CoV-2 spik protein (25–400 ng/mL) for 12, 24, and 48 h. At the end of the experiment, MTT (100 μL), 0.5 mg/mL with media, was added to each well, and the plate was incubated for 3 h. Excess MTT was then aspirated, and the formazan crystals formed were dissolved by 100 μL of dimethyl sulfoxide (DMSO). The absorbance, which was proportional to cell viability, was measured at 570 nm using a microplate reader (μQuant, Biotek Instruments, Winooski, VT, USA). The percentage of cell viability (%) was calculated as (A_{570} of treated cells/A_{570} of untreated cells) × 100.

2.5 | Quantitative Real-Time PCR

To analyze the expression of the SARS-CoV-2 spike's receptors like TLR4, ACE2, and GRP78, which are responsible for metabolomic alteration and inflammation, PMA-induced THP-1 cells were treated with spike protein (100 ng/mL), antcin A (20 μM), and dexamethasone (100 nM) for 12 h and then total mRNA was isolated using total RNA purification kit (GeneMark, New Taipei City, Taiwan). RNA was quantified with a NanoVue Plus spectrophotometer (GE Health Care Life Sciences, Chicago, IL, USA). 500 ng of the aliquot of total RNA was mixed with an oligo-dT (Life technology) and dNTP (Invitrogen). First-strand complementary DNA (cDNA) was generated by the SuperScript III reverse transcriptase kit (Invitrogen), and cDNA synthesized was quantified with a NanoVue Plus spectrophotometer (GE Health Care Life Sciences, Chicago, IL, USA). qPCR reactions performed quantified mRNA expression for genes of interest. The total reaction mixture contains 20 μl with 2 μg (2 μL) of cDNA, 2 μL (10 μM) of each primer, 10 μL of Power SYBR Green Master Mix (Applied Biosystems, Foster City, CA, USA), and the remaining DEPC-Treated water. The procedure for PCR was as follows: 95°C for 10 min, followed by 40 cycles of 95°C for 15 s, 60°C for 1 min, and 72°C for 30 s. The sequences of the specific primer, product size, gene ID, and accession variant number are summarized in Table 1. Sample normalization was performed using the human GAPDH endogenous control. The relative abundance of target mRNA for each sample was calculated from the $^{\Delta}$Ct values for the target and endogenous reference gene GAPDH using the 2^{Δ}Ct cycle threshold method.

2.6 | Sample preparation (metabolites)

After the different treatments, the culture media was aspirated and washed three times with PBS. Cells were harvested with 2 mL of trypsin and resuspended with 2 mL of fresh PBS. The cell suspension was transferred to a 2 mL centrifuge tube and centrifuged for 5 min at 500 × *g* at 4°C. The supernatant was aspirated, and the pellet obtained was stored at −80°C until the extraction step.

The pellet cells were sonicated on ice using the Ultrasonic Processor/UP-800 for 10 s at 60% intensity (Chrome tech, Apple Valley, CA, USA). Cold 90% methanol was used for the extraction of cellular metabolites, as described previously by (Dietmair, Timmins, Gray, Nielsen, & Kromer, 2010), with several modifications; unlike protein or RNA extraction, there is no available standard protocol to extract metabolites from the cells. A volume of 800 μL of extraction solvent (90% methanol) was added to the tube. The cell pellet was resuspended and vortexed on ice for 10 min. The cell suspensions were centrifuged at 10,000 × *g* for 15 min at 4°C. The supernatant was transferred into fresh tubes and stored at −80°C until further evaluation or continuation of drying sample for further evaluation. The supernatant was transferred to new tubes and dried in a vacuum drier. After the samples were dried, the samples were normalized for metabolic study. The obtained pellet cells were stored at −80°C for

TABLE 1 The sequences for used primers in the experiments

Gene ID	Accession number	Genes	Primers (5′—3′)	Product size
7,099	NM_005347	TLR4	For: CGAGGAAGAGAAGACACCAG Rev: CATCATCCTCACTGCTTCTGT	106 bp
59,272	NM_021804	ACE2	For: GCTGCTCAGTCCACCATTGAG Rev: GCTTCGTGGTTAAACTTGTCCAA	62 bp
3,309	NM_005347	GRP78	For: CTGTCCAGGCTGGTGTGCTCT Rev: CTTGGTAGGCACCACTGTGTTC	143 bp
2,597	NM_001256799	GAPDH	For: TCCTGGTATGACAACGAAT Rev: GGTCTCTCTCTTCCTCTTG	125 bp

Note: Gene ID, accession number, primer sequence, and product size of SARS-CoV-2 spike receptors genes Toll-like receptor 4 (TLR4), ACE2 angiotensin-converting enzyme 2 (ACE2), glucose-regulated protein 78 (GRP78), and glyceraldehyde-3-phosphate dehydrogenase (GAPDH). For: Forward; Rev: Reverse.

10991573, 0, Downloaded from https://onlinelibrary.wiley.com/doi/10.1002/ptr.7670 by Natl Chung Hsing University, Wiley Online Library on [22/11/2022]. See the Terms and Conditions (https://onlinelibrary.wiley.com/terms-and-conditions) on Wiley Online Library for rules of use; OA articles are governed by the applicable Creative Commons License

additional verification. All cell handling protocols were performed on ice unless otherwise noted. The detailed protocol is provided in Figure S3.

2.7 | Cell normalization

Cell metabolomes from different groups will be highly expected to be analyzed in cell-based metabolomics. Therefore, the sample amount needs to be normalized before NMR. Comparative measurements of the levels of metabolites found in different groups of cells. In this study, identical numbers of cells 2.5×10^6 cells/mL, were seeded in each 10 cm dish culture to guarantee that equal amounts would be used to harvest and extract the initial substance from each well (Luo, Gu, & Li, 2018). Three independent experiments were performed in triplicate.

2.8 | Preparation of samples for NMR analysis

As soon as the samples had been dried, the cell extract was re-suspended in 600 μL of the methanol-d4 solution containing the TSP (0.1% w/v). All samples were vortexed and transferred into 5 mm NMR tubes.

2.8.1 | NMR analysis

^{1}H-NMR analysis was conducted using a Bruker Advance III-400 NMR spectrometer (Bruker Corp, Billerica, MA, USA). The temperature was maintained at 25°C. Gradient shimming was achieved during the initial NMR data acquisition with the methanol-d4 as an internal lock. The chemical shifts referenced the internal standard TSP as zero chemical shifts. For every sample, 1,000 transient scans were obtained (Figures S4 and S5).

2.9 | Multivariate data analysis (MVDA) and metabolite characterization

The spectra were baseline, phased corrected, and a line broadening factor of 1.0 Hz was applied using TopSpin software (Bruker Corp). All spectra were binned and exported into an excel sheet for MVDA performed on the binned integrals of the ^{1}H-NMR data. The intensity or integral of the spectrum was determined by TopSpin based on TSP as 1. Further analysis was accomplished using MetaboAnalyst 5.0 (https://www.metaboanalyst.ca), web-based metabolomics analysis software with integrated R scripts. Missing values were estimated using k-nearest neighbors. Metabolites with missing values in 50% or more samples were excluded. Subsequently, the data were normalized by the sum of the total intensity and auto-log transformed for normalization data. In the subsequent two-sample *t*-test of each group, metabolites with a concentration change more significant than two-fold and a false discovery rate-adjusted *p*-value <.05 were considered significantly altered. The distance measure was Euclidean for hierarchical clustering analysis, and the clustering algorithm was ward. The groups are separated successfully using the partial least squares discriminant analysis (PLS-DA) machine learning analysis. The metabolite set enrichment analysis (MSEA) and metabolic pathway analysis (MetPA) 5.0 integrated metabolomics analysis for the over-represented metabolic pathways were performed to analyze the disease-related metabolic pathways. The metabolites identification was made to examine metabolites' chemical shifts from online databases, including the human metabolome database (https://hmdb.ca) and Biological Magnetic Resonance Data Bank (BMRB) (https://bmrb.io), and comparison with previous literature in detailed metabolites references (Table S1).

3 | RESULTS

3.1 | SARS-CoV-2 spike protein reduced the cell viability in PMA-induced THP-1 cells

We mainly subjected PMA-induced THP-1 cells to understand the metabolomic dysregulation by SARR-CoV-2 spike protein and the capability of antcin A rescue metabolomic disordered. Before investigating metabolomic profiles, we determined the cell viability of SARS-CoV-2 spike protein on THP-1 cells. PMA-induced THP-1 cells can be differentiated into a macrophage and mimic human MDMs (monocyte-derived macrophages). They represent the primary human host response to pathogen infection and link the immediate defense to the adaptive immune system. PMA-induced THP-1 cells were incubated with increasing concentrations (25–400 ng/mL) of spike protein for 12, 24, and 48 h, and cell viability was measured by MTT colorimetric assay. We found that spike protein displayed differential cytotoxicity to PMA-induced THP-1 cells, as shown in Figure 2a. More interestingly, 100 ng/mL of SARS-CoV-2 spike protein at 12 h reduced cell viability considerably compared to the control (Figure 2a). Incubation of PMA-induced THP-1 cells with 100 ng/mL for 12, 24, and 48 h reduced cell viability to 83.5%, 65.3%, and 48.7%, respectively (Figure 2a). High concentration and longer time showed that reduction in cell viability, which is more statistically significant.

In contrast, the high toxicity of the cells was not obtained enough for the metabolomic study. Secondly, the antcin A (10–50 μM) cytotoxicity and positive control dexamethasone was evaluated at a concentration of (25–400 nM) for 12, 24, and 48 h as dexamethasone and antcin A structurally resemble each other. As shown in Figure 2b and c, dexamethasone and antcin A do not display cytotoxicity to THP-1 cells. Thus, we can use the antcin A and dexamethasone to rescue the metabolomic dysregulated as it has not shown cytotoxicity to cells. According to cell viability results using the MTT assay, we selected SARS-CoV-2 spike protein (100 ng/mL for 12 h) for our further experiments as cells should not die less than 60% of cells for metabolomic activity study. We selected antcin A 20 μM and 100 nM of dexamethasone to regulate the metabolomic disordered as it is less differential. We suspended other concentrations for further investigation.

10991573, 0, Downloaded from https://onlinelibrary.wiley.com/doi/10.1002/ptr.7670 by Natl Chung Hsing University, Wiley Online Library on [22/11/2022]. See the Terms and Conditions (https://onlinelibrary.wiley.com/terms-and-conditions) on Wiley Online Library for rules of use; OA articles are governed by the applicable Creative Commons License

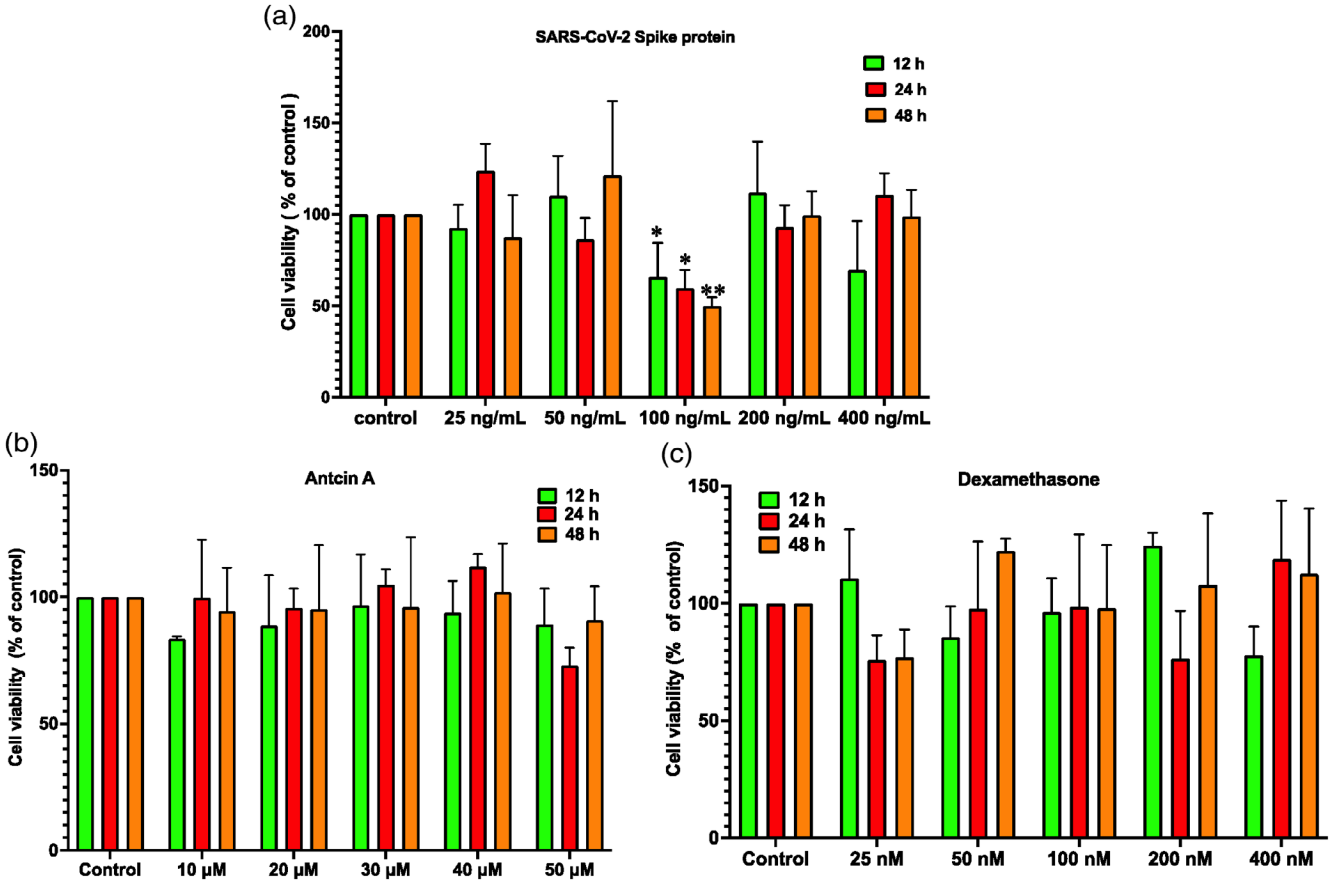

FIGURE 2 Cell viability effects of antcin, dexamethasone, and SARS-CoV-2 spike protein on PMA-induced THP-1 cells. (a) PMA-induced THP-1 cells were incubated with increasing concentrations of SARS-CoV-2 spike protein (25–400 ng/mL), (b) antcin A (10–50 µM), and (c) dexamethasone (25–400 nM) for 12, 24, and 48 h. The cell viability was determined by the MTT colorimetric assay as described in the materials and methods. Values represent the mean ± SD of three independent experiments. Statistical significance was set at $^{*}p < .05$, $^{**}p < .01$ compared to the treatment group versus the control group. Without asterisks, indicate the statistically non-significant

3.2 | The general spectral features of ^{1}H-NMR control and SARS-CoV-2 spike protein cells are similar

^{1}H-NMR analysis was utilized to evaluate the variations in metabolites profile in the control cells (Ctr) versus cells treated with SARS-CoV-2 spike (S) protein. The tentative identification of 46 metabolites detected in PMA-induced THP-1 cells is summarized in (Table 2). These metabolites were obtained from the human metabolome database https://hmdb.ca and biological magnetic resonance data bank (BMRB) https://bmrb.io and published literature comparing the chemical shift with the database (Table S3). Based on the obtained results, it is likely that cellular metabolites from control and SARS-CoV-2 spike protein treatment provide different information for the metabolite profiles in PMA-induced THP-1 (macrophage-like) cells, which provides SARS-CoV-2 spike protein might interrupt the cell metabolism. In general, relatively similar spectral features of ^{1}H-NMR were observed, while variations in the metabolite intensities can be seen in Figure S4. It is rather challenging to extract information regarding the metabolic shift in the studied cells based on the acquired NMR data. Therefore, we examined the MVDA by web-based MetaboAnalyst 5.0 https://www.metaboanalyst.ca to further explore the varying and similar metabolites profiles between control and spike protein treated in PMA-induced THP-1 cells. Different metabolic profiles between the control cells and cells treated with spike protein were observed by highlighting variations in the presence or absence of citrates, pyruvates, histidine, 3-methlyhistidine, and lactate (Table 2). Histidine, citrate, pyruvate, and 3-methylhistidine were not detected in SARS-CoV-2 spike protein-treated cells, whereas lactate and 3-methylhistidine were not detected in the control. As the alteration of the metabolomic pathway depends on metabolites, the SARS-CoV-2 spike protein might interfere with metabolomic pathways.

3.3 | Heatmap and partial least squares-discriminant analysis (PLS-DA) of control and SARS-CoV-2 spike protein-treated cells distinguished significantly

Multivariate data analysis was performed using MetaboAnalyst 5.0 to analyze the metabolite expression difference between the control and spike protein-treated groups. First, the data were visualized in the PLS-DA score plots to identify general metabolic trends between the

10991573, 0, Downloaded from https://onlinelibrary.wiley.com/doi/10.1002/ptr.7670 by Natl Chung Hsing University, Wiley Online Library on [22/11/2022]. See the Terms and Conditions (https://onlinelibrary.wiley.com/terms-and-conditions) on Wiley Online Library for rules of use; OA articles are governed by the applicable Creative Commons License

TABLE 2 The tentative assignments of ^{1}HNMR spectral signals from PMA-induced (THP-1) cells for control (without SARS-CoV-2 spike protein treatment) and treatment with SARS-CoV-2 spike protein

ID	Metabolites	Chemical shift (ppm)	Control	Spike
1	Phosphoenolpyruvic acid	5.32 (s), 5.38 (s)	+	+
2	α-Glactatose	5.23(dd), 5.36 (d)	+	+
3	Histidine	4.01 (dd), 3.15(dd)	+	–
4	Aspargine	4.01 (dd), 2.86(dd)	+	+
5	Phenylalanine	3.99 (dd), 3.30(dd), 3.14 (dd), 3.29(dd)	+	+
6	Phosphoethanolamine	3.98(m)	+	+
7	Alanine	3.79(q)	+	+
8	α-Glucose	3.73(m), 3.54(m), 3.64 (m)	+	+
9	Valine	3.62(t) 0.98(d), 3.61(t) 0.97(d)	+	+
10	Phosphocholine	3.61(t), 3.22(d)	+	+
11	Myo-inositol	3.59(t), 3.12(s), 3.51(dd)	+	+
12	Threonine	3.59(d), 2.33(d)	+	+
13	Glycine	3.57(s)	+	+
14	β-Glucose	3.46–3.48(d)	+	+
15	Proline	3.34(m), 2.35(m), 2.06(m)	+	+
16	Cysteamine	3.22(d), 3.11(dd)	+	+
17	Glycero-2-phosphocholine	3.23(d), 3.16 (s)	+	+
18	Ethanolamine	3.15(dd), 3.12(t)	+	+
19	Lysine	3.02(m)	+	+
20	Creatine	3.02(s)	+	+
21	Asparagine	2.84(dd), 2.82(dd), 2.98(m)	+	+
22	Hypotuarine	2.65(s)	+	+
23	Citrate	2.57(dd)	+	–
24	Glutamine	2.44(m), 2.43(m),	+	+
25	Succinate	2.45(s), 2.65 (s)	+	+
26	Pyruvate	2.35(s)	+	–
27	3-hyroxybutyrate	2.31(dd), 4.16 (d)	+	+
28	Acetoacetate	2.29(s)	+	+
29	Methyl-succinate	2.13(d), 1.10(d)	+	+
30	Glutamate	2.12(m), 2.08(m)	+	+
31	Methionine	2.12(s), 2.10(s) 2.11(s)	+	+
32	*N,N*-dimethylglycine	2.02(s), 2.92 (s)	+	+
33	Quinic acid	1.88(m)	+	+
34	Fatty acid c	1.59(m)	+	+
35	n-Heptanoate	1.30(m)	+	+
36	Fatty acid a	1.28(m)	+	+
37	Isoleucine	1.01(d), 0,94(dd)	+	+
38	Butyrate	0.90(t)	+	+
39	2-Hyroxybutyrate	0.89(t)	+	+
40	Carnitine	4.57(m), 3.22(s)	+	+
41	3-Methylhistidine	3.30(q)	–	–
42	Lactate	1.32(d)	–	+
43	Malonate	3.12(s)	+	+
44	Leucine	0.97(d), 0.91(d), 0.95 (d)	+	+
45	Aspartate	2.84(dd)	+	+
46	Canadine	3.32 (s)	+	+

Note: The representation: singlet (s), doublet (d), triplet (t), and multiplet (m). (+): metabolites in the study group, (–): not present in the study group. Citrate, pyruvate, and histidine were not found in spike protein-treated cells. Methyl-histamine and lactate are not present in the control group. These metabolites are obtained from literature, Human metabolome databases https://hmdb.ca, and Biological Magnetic Resonance Data Bank (BMRB) https://bmrb.io. The data are reported in three independent experiments.

10991573, 0, Downloaded from https://onlinelibrary.wiley.com/doi/10.1002/ptr.7670 by Natl Chung Hsing University, Wiley Online Library on [22/11/2022]. See the Terms and Conditions (https://onlinelibrary.wiley.com/terms-and-conditions) on Wiley Online Library for rules of use; OA articles are governed by the applicable Creative Commons License

two samples. SARS-CoV-2-spike protein-treated group (spike) and non-treated group (Ctr) were separated successfully by components 1 (37.9%) and 2 (17.2%) in the PLS-DA machine learning analysis, as shown in Figure 3a. PLS-DA of the whole cellular metabolites demonstrated two distinct clusters established (Figure 3a). The high reproducibility of the prepared biological replicates is based on proximity, as depicted in the PLS-DA score plot. Two clusters, representing control and spike-treated groups, were spotted separately by indicating green as the control and red as a spike protein treatment. Among the metabolites that contributed to the segregation of control from spike-protein treated groups were included glycerol-phosphocholine (GPC) (δ3.22 (d), δ3.16 (s)), glycine (δ 3.57 (s)), canadine (δ3.32 (s)), sarcosine (δ3.62), ethanolamine (δ, 3.14(dd), 3.12 (t)), β-glucose (δ 3.46–3.48(d)), phosphoenolpyruvic acid (PEP) (δ5.32 (s), 5.38 (s)), glutamine (δ 2.44 (m), 2.43 (m)), glutamate (δ 2.12(m), 2.08(m)), succinate (δ 2.45(s), 2.65 (s)), and *N*,*N*-dimethylglycine (DMG), (δ 2.92 (m)). It is provided that the variable importance in the projection (VIP) is more than 1 score in Figure 3b. To further confirm, we applied heatmap analysis using Ward's method. The relative concentrations of the identified metabolites were calculated and compared among the two samples in Figure 4. The metabolite variations are represented by different shades of color, with red and blue being the highest and lowest amounts of the two sample groups. The control group revealed distinctively higher cellular metabolites from the SARS-CoV-2 spike protein group, as indicated by PLS-DA's VIP score in Figure 3b. The ranking of the VIP score metabolites shows that the heat map also corresponds to the PLS-DA score.

3.4 | Statistical analysis of the metabolite's expression level shows significant differences in the spike-treated cells and control

We observed relatively similar spectral features of ^{1}H-NMR in the control and spike protein-treated cells. MetaboAnalyst 5.0 performed the metabolite expression level. In this work, the fold change (FC) threshold was set at two, the comparison was made for the control versus the spike protein-treated group, and the emphasis focused on metabolites with a VIP > 1.0, as revealed in Figure 3b. The number of pairs with a consistent change above the desired FC threshold was initially determined for paired analysis. If the given number surpasses the specified count threshold, the variable is considered significant (Table S2), and *p*-value is lower than .05. As shown in Figure 5, eight metabolites demonstrated significant trends in metabolite changes, including GPC, glycine, DMG, sarcosine, canadine, PEP, glutamate, and glutamine. SARS-CoV-2 spike protein-treated cells demonstrated that GPC, glycine, sarcosine, and canadine are remarkably reduced compared to the control in Figure 5. In contrast, PEP, glutamate,

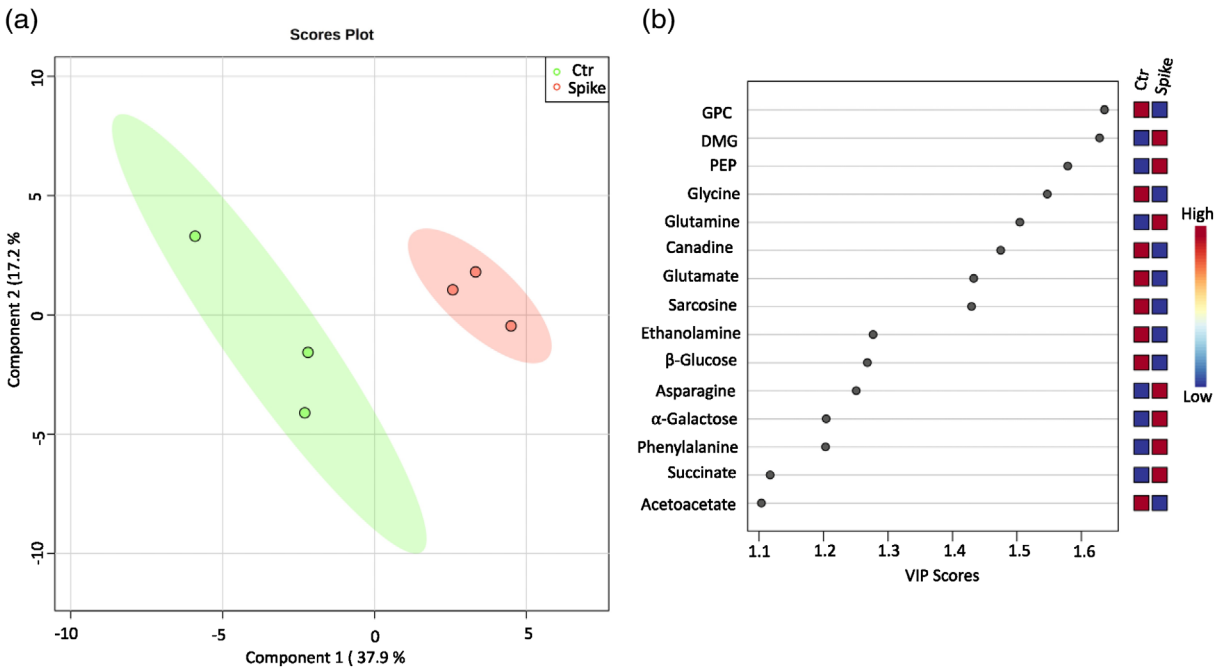

FIGURE 3 SARS-CoV-2 spike protein treated groups separate successfully from the non-treated group. (a) SARS-CoV-2 spike-treated group (Spike) and non-treated group (Ctr) were separated successfully by components 1 (37.9%) and 2 (17.2%) in the partial least squares discriminant analysis (PLS-DA) machine learning analysis. The green dots represented without treatment of SARS-CoV-2 spike protein (Ctr), and the red dots represented the cells treated with SAR-CoV-2-spike protein (Spike) in the two-dimensional PLS-DA score plots. All the experiments have been done at least in triplicate. Thus, spike-treated metabolites were distinguished from the control groups. (b) Variable importance in projection (VIP) scores of the spike-treated and non-treated metabolites by proton nuclear magnetic resonance analysis (^{1}H-NMR) (number of experiments = 3). Fifteen important metabolites were selected based on the VIP score > 1.1 as the VIP score was based on the PLS-DA model. The heat map with red or blue squares on the right indicates a high and low abundance ratio of the corresponding metabolites in spike and control groups. Glycerophosphocholine (GPC), *N*,*N*-dimethylglycine (DMG), phosphoenolpyruvic acid (PEP), glycine, glutamine, canadine, glutamate, sarcosine, ethanolamine, β-glucose, asparagine, α-galactose, phenylalanine, succinate, and acetoacetate. The data are reported as mean ± SD of three independent experiments

10991573, 0, Downloaded from https://onlinelibrary.wiley.com/doi/10.1002/ptr.7670 by Natl Chung Hsing University, Wiley Online Library on [22/11/2022]. See the Terms and Conditions (https://onlinelibrary.wiley.com/terms-and-conditions) on Wiley Online Library for rules of use; OA articles are governed by the applicable Creative Commons License

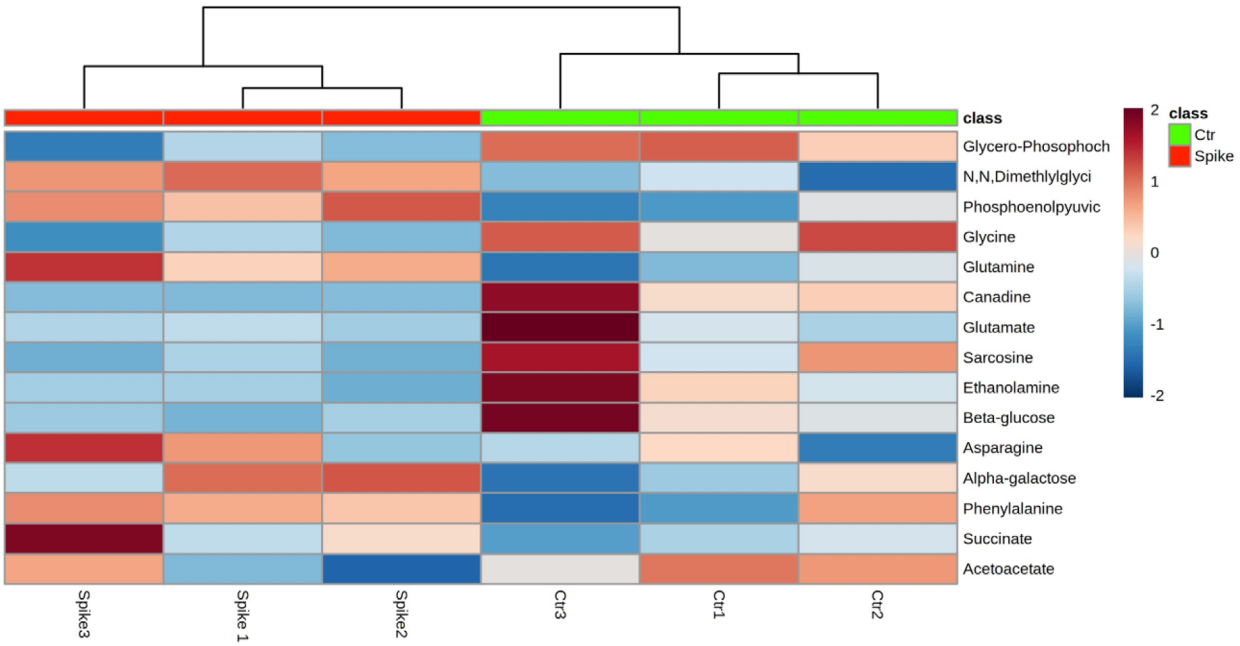

FIGURE 4 Heat map selected PLS-DA VIP metabolite expression levels. This heatmap visualizes the top 15 metabolites from the control and SARS-CoV-2 spike protein-treated groups. The degree of variation was color-coded, ranging from dark red (with a positive value of 2) to dark blue (with a negative value of 2), representing the highest computed ratio of metabolites to the lowest. The examined group of cells includes; green boxes that are non-treatment of SARS-CoV-2 spike control (Ctr) sample; red boxes are treated with SARS-CoV-2 spike protein treated groups. Metabolites are represented in each row, while a column represents each replicate. Ward's method and colored boxes were generated using MetaboAnalyst 5.0. The data are reported as mean ± SD of three independent experiments

glutamine, and DMG are significantly increased compared to control in the spike protein-treated cells, as shown in Figure 5. It is also worth noting that the absolute changes in metabolites observed for metabolites like glutamine and glycine are associated with inflammation and COVID-19 (Cengiz et al., 2020; Li, 2020). Therefore, understanding the differential metabolites protects from COVID-19 severity. Overall, this result indicates that the SARS-CoV-2 spike protein interferes with metabolomics related to inflammation in PMA-induced THP-1 as metabolic activity relies on the expression level of metabolites in the specific pathway. An orthogonal partial least squares discriminant analysis (OPLS- DA) model was then performed to minimize the possible influence of between-group variability and metabolomics screen differences among the two groups. Sevenfold cross-validation was applied to estimate the predictive ability of the OPLS-DA models. The parameters for classifying the control versus spike protein-treated group for the cell extract samples, respectively. Both models were obtained with one predictive and one orthogonal component respectively; R2X = 0.31, R2Y = 0.869, Q2 = 0.57 R2X = 0.22, R2Y = 0.10, Q2 = 0.03 as shown in Figure S6, which demonstrated acceptable goodness of fit and high-quality predictability.

3.5 | Potential biomarkers to detect the presence of the SAR-CoV-2 spike protein in the host cells

To determine the practicality of using biomarkers to assess the presence of the SARS-CoV-2 spike protein in the host cells, we examined the metabolites from control (Ctr) and SARS-CoV-2 spike protein-treated cells. The color-coded significant metabolites VIP plot (Figure 3b) identified valuable metabolites distinguished between the control and SARS-CoV-2 spike protein-treated groups. It can be targeted those metabolites by the therapeutic drug or natural products. Both univariate and multivariate exhibited increased DMG, PEP, glutamine, glutamate, asparagine, α-galactose, phenylalanine, and succinate spike-treated group compared with the control group. In contrast, GPC, glycine, canadine, and sarcosine are tremendously decreased compared to the control group in spike treated group. However, ethanolamine, β-glucose, and acetoacetate are not significantly reduced, as shown in Figure 3b. Potential biomarkers were validated using MetaboAnalyst 5.0 (Chong, Wishart, & Xia, 2019). It is one of the powerful learning machines for metabolomic studies that offers various statistical analyses. The biomarker discovery and validation are involved in three steps; (1) data preprocessing, (2) biomarker selection, and (3) model performance evaluation. After data processing, five metabolites were selected: glutamate, glycine, PEP, glutamine, DMG, and GPC, based on fold change, *p*-value, and area under the curve (AUC), which is more than 95%. This analysis revealed receiver operating characteristic curve (ROC) curves for the individual biomarker panel models and associated AUC values, fold change, and *p*-value that control groups versus the SARS-CoV-2 spike protein treated group. PLS-DA generated these top 6 ROC models with an increasing number of variables. AUC (CI, 95%) confidence intervals; PLS-DA, Var, number of variables included in the model as shown in Figure 6a. It showed an AUC of 0.78–1 (95% CI 0.90–1) to predict the infection of SARS-

10991573, 0, Downloaded from https://onlinelibrary.wiley.com/doi/10.1002/ptr.7670 by Natl Chung Hsing University, Wiley Online Library on [22/11/2022]. See the Terms and Conditions (https://onlinelibrary.wiley.com/terms-and-conditions) on Wiley Online Library for rules of use; OA articles are governed by the applicable Creative Commons License

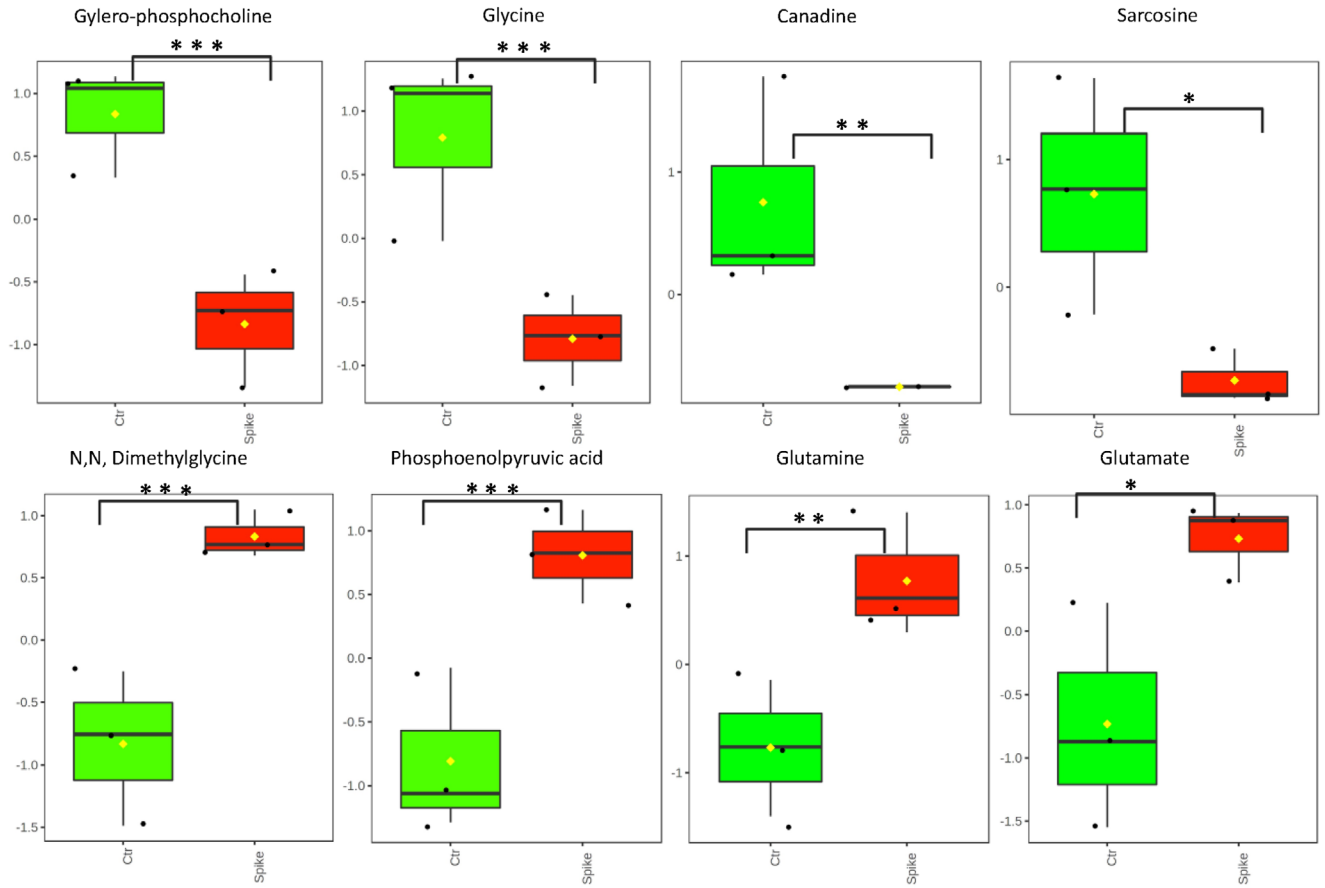

FIGURE 5 Each metabolite's expression level changes with respect to the control group. Eight metabolites were found with significant fold change, with *p*-values lower than .5. Green boxes are non-treatment of SARS-CoV-2 spike control (Ctr) sample, and red boxes are treated with SARS-CoV-2-spike (Spike) protein samples of 100 ng/mL for 12 h. Box-and-Whisker plots were plotted by using MetaboAnalyst5.0. https://www.metaboanalyst.ca. Glycero-phosphocholine (GPC), glycine, sarcosine, and canadine are significantly reduced in spike-treated cells compared to the control. In contrast, the expression level of phosphoenolpyruvic acid (PEP), *N*,*N*-dimethylglycine (DMG), glutamate, and glutamine are significantly increased compared to control in the spike-treated group. The chemical shifts in bold were used to calculate integrals and *p*-values by comparing them with control groups. The data are reported as mean ± SD of three independent experiments. $^{*}p < .05$, $^{**}p < .01$ and $^{***}p < .001$ were significantly different from control versus SARS-CoV-2 spike protein treatment groups

CoV-2 spike into the cells. This also indicated that AUCs ranged from 0.99 (95% CI 0.00–0.99; 46 variables) to 0.88 (95% CI 0.00–0.99; 5 variables), each being statistically significant. More importantly, it shows that predictive accuracies of the models with an increasing number of features are better and more reliable, as shown in Figure 6b because the inclusion of more variables into a model improved the discriminatory power of the results. Thus, this result shows that the above-selected metabolites can be used as a potential biomarker by increasing the variable number in the samples.

3.6 | The most metabolites alteration in SARS-CoV-2 spike protein rescue by antcin a

It has been well defined that antcin A exhibited a prophylactic activity (Chen et al., 2011). In addition, it reduced the angiotensin-converting enzyme (ACE2) expression in the HT-29 cells (Kumar et al., 2021), which can be used as natural therapeutic for anti-COVID-19. Most altered metabolites are related to the inflammatory response, including GPC, glycine, sarcosine, acetoacetate, DMG, and glutamine. This allows us to investigate the effect of antcin A on metabolomic altered by SARS-CoV-2 spike protein in THP-1 cells and dexamethasone as a positive control because it has been used to treat COVID-19 patients (Sharun, Tiwari, Dhama, & Dhama, 2020) and structurally similar each other. PMA-induced THP-1 cells were treated as follows; control; SARS-CoV-2 spike protein (100 ng/mL); dexamethasone (100 nM); antcin A (20 μM); S + Antcin A; S + Dex; and these were maintained under 5% CO_2 at 37°C for 12 h. We have performed ^{1}H-NMR and showed ^{1}H-NMR spectra (Figure S5). MetaboAnalyst 5.0 to analyze the metabolite expression level revealed that 14 metabolites were significantly different, which *p*-value being lower than .05 different, including isoleucine, α-glucose, malonate, creatine, α-galactose, acetoacetate, β-glucose, methionine, PEP, canadine, glutamate, glutamine, ethanolamine, and phenylalanine. The antcin A-treated group showed significantly increased metabolites like isoleucine, α-glucose, α-galactose, and methionine (Figure 7a). The increasing glucose in the cells would enhance their viability (Han et al., 2015). This finding suggests that antcin A can boost metabolites associated with anti-viral

10991573, 0, Downloaded from https://onlinelibrary.wiley.com/doi/10.1002/ptr.7670 by Natl Chung Hsing University, Wiley Online Library on [22/11/2022]. See the Terms and Conditions (https://onlinelibrary.wiley.com/terms-and-conditions) on Wiley Online Library for rules of use; OA articles are governed by the applicable Creative Commons License

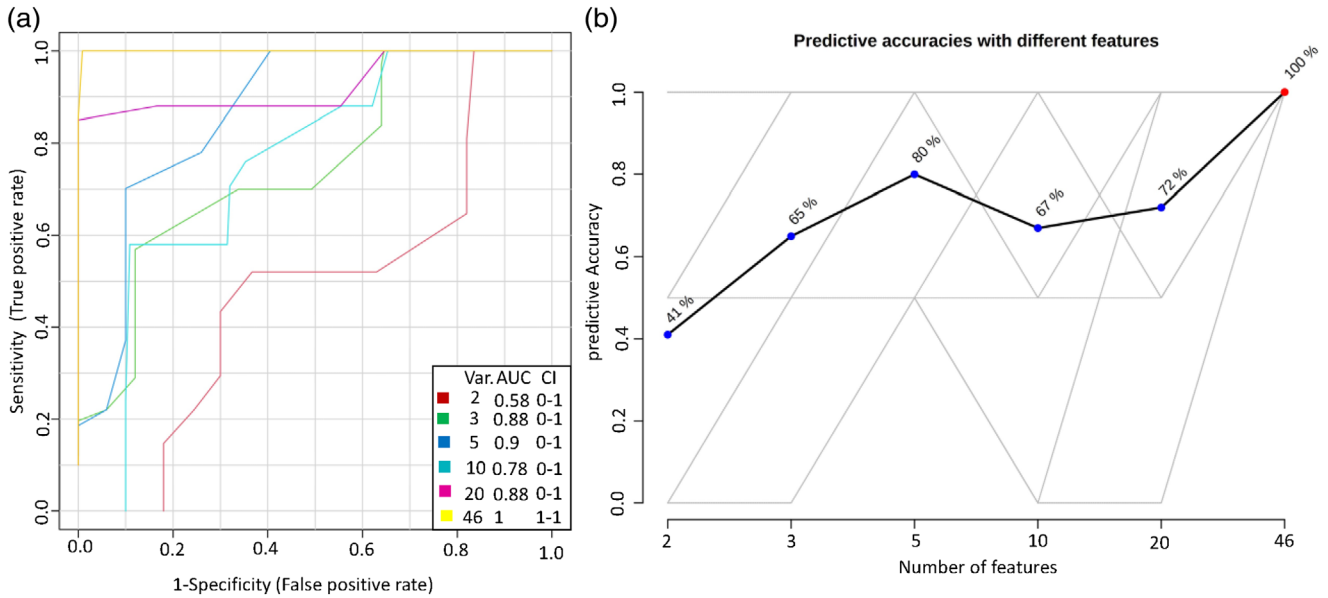

FIGURE 6 The potential biomarkers for the infection of SARS-CoV-2 spike in the cells. (a) six metabolites were selected: glutamate, glycine, phosphoenolpyruvic acid, glutamine, *N*,*N*-dimethylglycine, and glycerophosphocholine based on the fold change, *p*-value, and area under the curve (AUC), which is more than 95% using MetaboAnalyst5.0. It revealed that the individual biomarker panel models' receiver operating characteristic curve (ROC) curves and associated AUC values, fold change, and *p*-value that control groups versus SARS-CoV-2 spike protein treated group. It consists of six number of variables (Var); AUC at 0.58 (Var- 2), confidence interval (CI; 0–1), AUC at 0.88 (Var;3), (CI;01), AUC at 0.9 (Var;5), (CI;0–1), AUC at 78, (Var; 10), (CI;0–1), AUC at 0.88 (Var;20), (CI;0–1), and AUC at 0.99 (Var;46), (CI;1–1). It shows that a greater number of variables has better accuracy prediction. (b), Predictive accuracies of the models are based on the number of variables. This prediction accuracy was tested with associated AUC, sensitivity, and specificity. For example, Var; 20, sensitivity is more than 80%, whereas its specificity is lower than 60%. However, Var;46, sensitivity is more than 90% also specificity is more than 90%. Thus, this model shows that Predictive accuracies increased with the inclusion of several features. The data are reported as mean ± SD of three independent experiments

infection and antiinflammation. We also found that Antcin A treatment does not affect cell viability compared to the control. Amino acids like isoleucine and methionine also increased significantly because the utilization of these amino acids might fuel up the energy in antcin A-treated cells via the TCA cycle and glycolysis to produce more ATP (Anderson, Mucka, Kern, & Feng, 2018). More interestingly, we observed that the presence of antcin A in SARS-CoV-2 spike protein-treated cells reverses the spike's action on metabolite expression. It is highly similar to the control group, including PEP, glutamine, glutamate, ethanolamine, and phenylalanine are shown in Figure 7b. For example, PEP was significantly increased when cells were treated with a spike protein-treated compared to the control. However, PEP was reduced when cells were treated with antcin A in spike-treated cells, as shown in Figure 7b. At the same time, glutamine reduced in the presence of the antcin A in the spike-treated cells implies that antcin A rescues the metabolites altered by SARS-CoV-2 spike protein and reduces the inflammation (Figure 7b). However, dexamethasone-treated only, dexamethasone in the spike treated had not changed metabolic concentration compared with the control and spike protein-treated group (Figure 7b). Still, when cells are treated with antcin A only, the concentration of PEP is similar to the control. In addition, the treatment of dexamethasone in spike protein-treated did not change. It remained at almost the same concentration metabolites compared with control which shows that dexamethasone has an associated reduction of the destructive cytokine produced in COVID-19 patients, whereas not related to the metabolic correction (Sharun et al., 2020) for COVID-19 treatment. Therefore, the metabolic profile was not significantly changed upon dexamethasone treatment in PMA-induced THP-1 cells (Figure 7a and b). More importantly, antcin A reversed the action of the SARS-CoV-2 spike protein in PMA-induced THP-1 cells, which indicates that antcin A could be used for metabolic correction that alteration mediated by the SARS-CoV-2 spike protein, whereas dexamethasone has failed to do so. This finding suggests that antcin A could potentially treat metabolic alteration by spike protein.

3.7 | Antcin a regulates metabolomic alteration that may not occur via the reduction of expression of ACE2 and TLR4

Although recent attempts to discover novel SARS-CoV-2 spike protein does not activate only the angiotensin-converting enzyme 2 (ACE2), it can directly interact with Toll-like receptor 4 (TLR4) and glucose-regulated protein-78 (GRP78) and produce pro-inflammatory cytokines, such as IL-6, and TNF-α, IL-8, and IL-1β (Nassar et al., 2021; Zhao et al., 2021). Eventually, it causes severity and death in COVID-19 patients (Hojyo et al., 2020). It allows us to investigate the detailed mechanism of the metabolomic alteration as we have observed cell viability sufficiently reduced in the presence of the

10991573, 0, Downloaded from https://onlinelibrary.wiley.com/doi/10.1002/ptr.7670 by Natl Chung Hsing University, Wiley Online Library on [22/11/2022]. See the Terms and Conditions (https://onlinelibrary.wiley.com/terms-and-conditions) on Wiley Online Library for rules of use; OA articles are governed by the applicable Creative Commons License

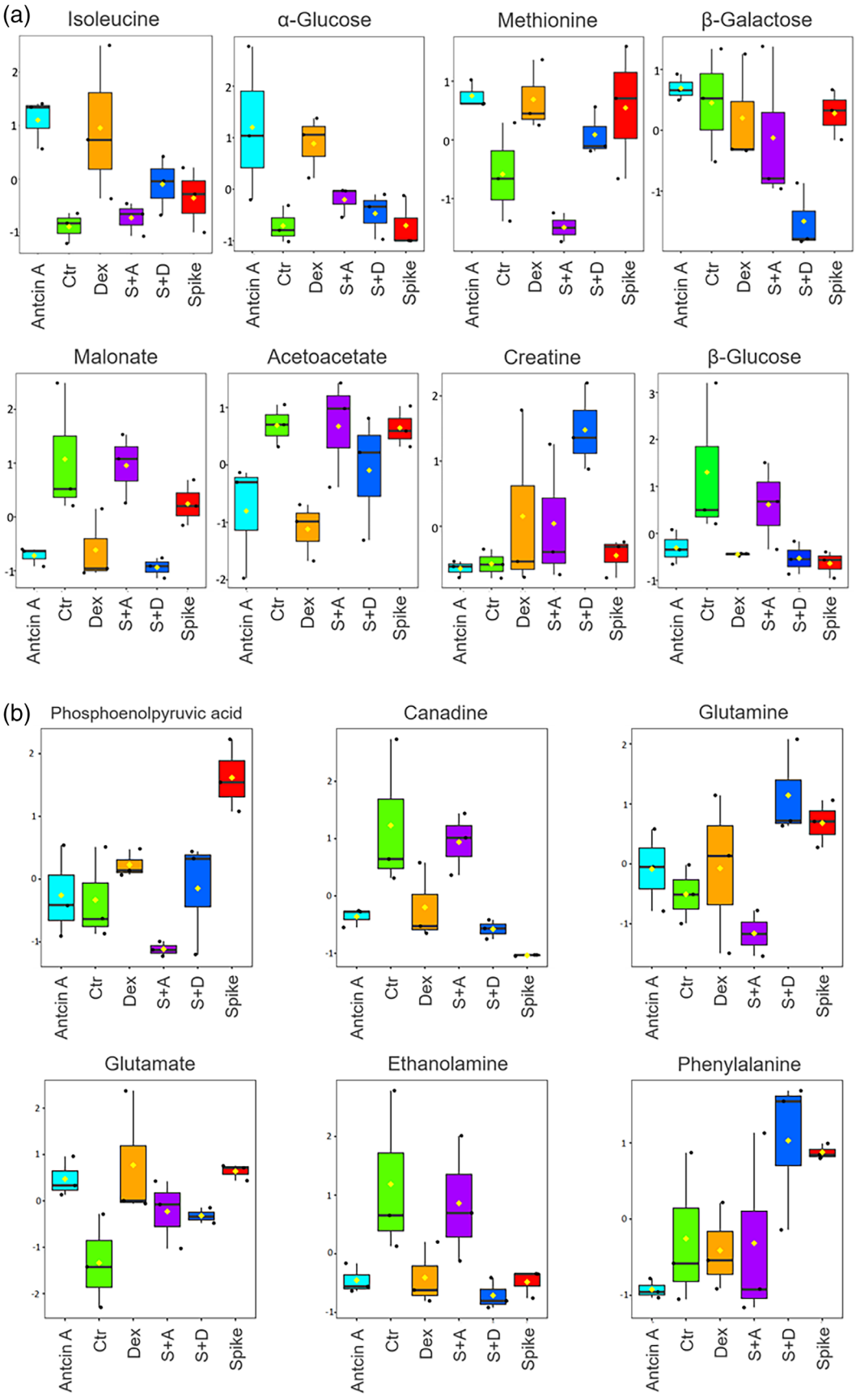

FIGURE 7 Legend on next page.

10991573, 0, Downloaded from https://onlinelibrary.wiley.com/doi/10.1002/ptr.7670 by Natl Chung Hsing University, Wiley Online Library on [22/11/2022]. See the Terms and Conditions (https://onlinelibrary.wiley.com/terms-and-conditions) on Wiley Online Library for rules of use; OA articles are governed by the applicable Creative Commons License

100 ng/mL of SARS-CoV-2 spike protein compared to control and altered metabolomic profiles in PMA-induced THP-1 cells. The metabolomic alteration was corrected by the presence of antcin A in PMA-induced THP-1 cells, whereas dexamethasone failed to modulate. Thus, we tested three different receptors for SARS-COV-2 spike protein: ACE2, TLR4, and GRP78 which mediated inflammation. We treated cells with 100 ng/mL spike protein for 12 h. As shown in (Figure 8a–c), the expression of TLR4, ACE2, and GRP78 increased significantly, suggesting the reduction of cell viability is due to increased expression of ACE2, TLR4, and GRP78 which interfere with a cellular metabolomic profile in the host cells.

Interestingly, the expression levels of TLR4 and ACE2 were significantly decreased in the presence of the antcin A and dexamethasone in the spike protein-treated cells, making them similar to the control (Figure 8a–c). At the same time, GRP78 was not reduced in the presence of antcin A, implying that GRP78 is not responsible for metabolomic alteration. However, without treating spike protein in PMA-induced THP-1 cells, antcin A and dexamethasone have not reduced the mRNA expression of the ACE2 and TLR4, and GRP78, which implies that both antcin A and dexamethasone do not interfere with normal cells and cell viability in PMA-induced THP-1 cells because ACE2 regulates physiological counterbalance providing homeostatic regulation of the cells and TLR4 represents the first line of defense against infections. The metabolomic alteration may not be through activation of ACE2 and TLR4, as we observed that antcin A rescued the metabolomic alter, mediated by the SARS-CoV-2 spike protein. Still, dexamethasone failed to do it. However, both dexamethasone and antcin A reduced the expression of spike protein receptors such as TLR4 and ACE2. In contrast, dexamethasone cannot rescue the metabolomic disordered. Thus, the natural compounds derived from fruiting bodies of *T. camphoratus* are not only restricted to inhibition of ACE2 and TLR4 expression and anti-inflammation; it could rescue the metabolomic alteration that is not capable of the dexamethasone. Thus, antcin A can be used to reduce the expression of spike protein receptors and rescue metabolomic disorders.

3.8 | The treatment of SARS-CoV-2 spike protein altered 10 metabolic pathways, which were corrected by antcin A

The alteration of the metabolic pathway is caused by the change in metabolite expression level in the specific metabolism. A study demonstrated that unbalanced succinate in the cells led to metabolic stress. Thus, a supplement of succinate enhances the TCA cycle, leading to higher ATP production and reduced inflammation (Jalloh et al., 2017). Therefore, it is essential to understand the link between those metabolites with specific metabolomic pathways. Metabolomic pathway analysis was performed using (MetPA) to reveal the most relevant pathways related to enrichment analysis based on the target metabolites (Chong et al., 2019). The metabolites (VIP >1.0) and *p*-value <.05 from the cells are subjected to quantitative metabolite set enrichment analysis (MSEA) aimed to characterize the metabolic pathways that were by the 15 metabolites. We found 14 metabolisms whose *p*-value is lower than .05. The MSEA analysis facilitates the characterization and understanding of the metabolic shifts in the human metabolome in a biologically relevant framework. Several metabolisms in control and spike protein-treated cells were significantly modified, including energy metabolism, which compromised the glycolysis and Warburg effect. Also, glutamate metabolism contains specific amino acids like glutamine, glutamate, and carbohydrate compounds like PEP, as detailed in Figure 9a. Eventually, metabolisms are also affected by metabolic pathways. Furthermore, the potential target pathway was determined using pathway topology analysis and evaluated for an impact value above 0.1. For this impact value, we found ten possible target pathways, namely (1) synthesis and degradation of ketone bodies, (2) $_D$-glutamine and $_D$-glutamate metabolism, (3) phenylalanine, tyrosine, and tryptophan biosynthesis, (4) glutathione metabolism, (5) alanine, aspartate, and glutamate metabolism, (6) phenylalanine metabolism, (7) glycine, serine and threonine metabolism, (8) arginine and proline metabolism, (9) butanoate metabolism, and (10) glycolysis/gluconeogenesis, related to 14 of the metabolites identified in this research which includes isoleucine, α-glucose, malonate, creatine, α-galactose, acetoacetate, β-glucose, methionine, PEP, canadine, glutamate, glutamine, ethanolamine, and phenylalanine. Most of these altered metabolites are due to SARS-CoV-2 spike protein are corrected by antcin A in PMA-induced THP-1 cells after 12 h. The ten pathways, which included more than one target metabolism, were disrupted across the spike protein-treated group, as shown in Figure 9b, corrected by treating the natural compound sufficiently. We found that $_D$-glutamine and $_D$-glutamate metabolism have the highest impact score. We significantly changed that is due to the alteration of expression of the glutamine and glutamate metabolites under SARS-CoV-2 spike protein treatment in the cells. However, it was reversed in the presence of the antcin A in PMA-induced THP-1 cells. More interestingly, all the above ten metabolic pathways were

FIGURE 7 The expression level change of each metabolite with respect to the Ctr group and SARS-CoV-2 spike treated in THP-1 cells. The expression level change of each metabolite compared with the Ctr group and SAR-CoV-2 treated metabolites. 14 metabolites were found with significant fold change, and *p*-values are lower than 0.5. Green boxes are non-treatment of SARS-CoV-2 spike control (Ctr) sample, and red boxes are treated with SARS-CoV-2 spike (spike). Purple boxes are the treatment of 20 μM of antcin A in 100 ng/mL of spike-treated (S + A) samples. Blue boxes are treatments of 100 nM of Dexamethasone (Dex) in the spike-treated (S + D) samples. Orange boxes are treated with only 100 nM of Dex, and turquoise boxes are only treated with 100 nM of Dex. All models were treated for 12 h in a 5% CO_2 incubator at 37°C. Box-and-Whisker plots were plotted by using MetaboAnalyst5.0 https://www.metaboanalyst.ca. The chemical shifts in bold were used to calculate integrals and *p*-values, compared with the control and spike-treated groups, $p < .05$ using MetaboAnalyst5.0 https://www.metaboanalyst. The data are reported as mean ± SD of three independent experiments

10991573, 0, Downloaded from https://onlinelibrary.wiley.com/doi/10.1002/ptr.7670 by Natl Chung Hsing University, Wiley Online Library on [22/11/2022]. See the Terms and Conditions (https://onlinelibrary.wiley.com/terms-and-conditions) on Wiley Online Library for rules of use; OA articles are governed by the applicable Creative Commons License

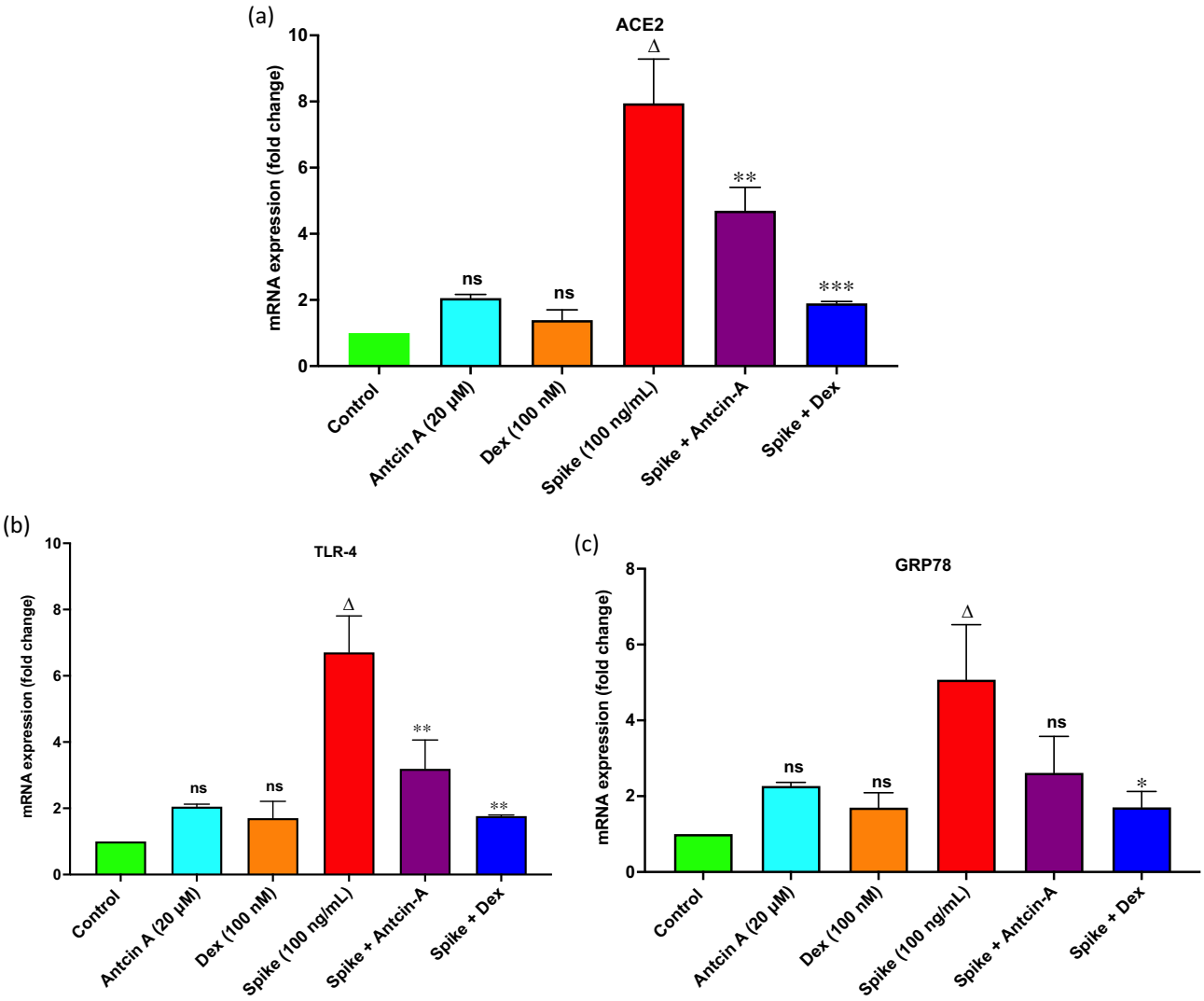

FIGURE 8 The mRNA expression level of the receptors upon treatment of SARS-CoV-2 spike and antcin A in the PMA-induced THP-1 cell. (a) It checked mRNA expression of the angiotensin-converting enzyme-2 (ACE2), (b) toll-like receptor-4 (TLR-4), and (c) glucose-regulated protein78 (GRP78) from PMA-induced THP-1 cells which were treated with 100 ng/mL of SARS-CoV-2-S, 20 μM of antcin A, 100 nM of dexamethasone, and 20 μM of antcin A in 100 ng/mL of spike-treated (Spike + A) samples. The treatments of 100 nM of dexamethasone (Dex) in the spike-treated (Spike + Dex) samples and non-treatment control. All treatments are incubated in a 5% CO_2 incubator at 37°C for 12 h. The column graph was plotted by using GraphPad Prism 9.0. mRNA levels were normalized to the expression of GAPDH, then the expression of genes of each sample was calculated compared with the control. Statistical significance was set at $^{\Delta}p < .001$ compared to control versus SARS-CoV-2 spike protein treated and $^{*}p < .05$, $^{**}p < .01$, $^{***}P < .001$ were significantly which compared to spike treated versus S + A, S + D, and ns represents insignificant. The data are reported as mean ± SD of three independent experiments

altered due to changes in the expression of metabolites and corrected by antcin A.

4 | DISCUSSION

COVID-19 is still an ongoing global pandemic and not a specific therapy well established. In COVID-19 patients, the cause of death is significantly related to cytokine storm production via activation of the ACE2 and TLR4 (Hojyo et al., 2020; Zhao et al., 2021). Recent studies revealed that plasma metabolic abnormalities are another hallmark of severity in COVID-19 patients (Wu et al., 2020). Despite this, the effect of SARS-CoV-2 spike protein on cellular metabolism is poorly understood. We have applied the ^{1}H-NMR-based metabolomic approach for this study. It presents a significant analytical challenge because, unlike genomic and proteomic methods to measure molecules with disparate physical properties (e.g., ranging in polarity from very water-soluble organic acids to very nonpolar lipids (Jacob, Lopata, Dasouki, & Abdel Rahman, 2019)). Thus, even only the spike protein of SARS-CoV-2 alters the expression of metabolites in host cells. Most altered metabolites were highly associated with inflammation, including GPC, DMG, sarcosine, glycine, and ethanolamine, upon

10991573, 0, Downloaded from https://onlinelibrary.wiley.com/doi/10.1002/ptr.7670 by Natl Chung Hsing University, Wiley Online Library on [22/11/2022]. See the Terms and Conditions (https://onlinelibrary.wiley.com/terms-and-conditions) on Wiley Online Library for rules of use; OA articles are governed by the applicable Creative Commons License

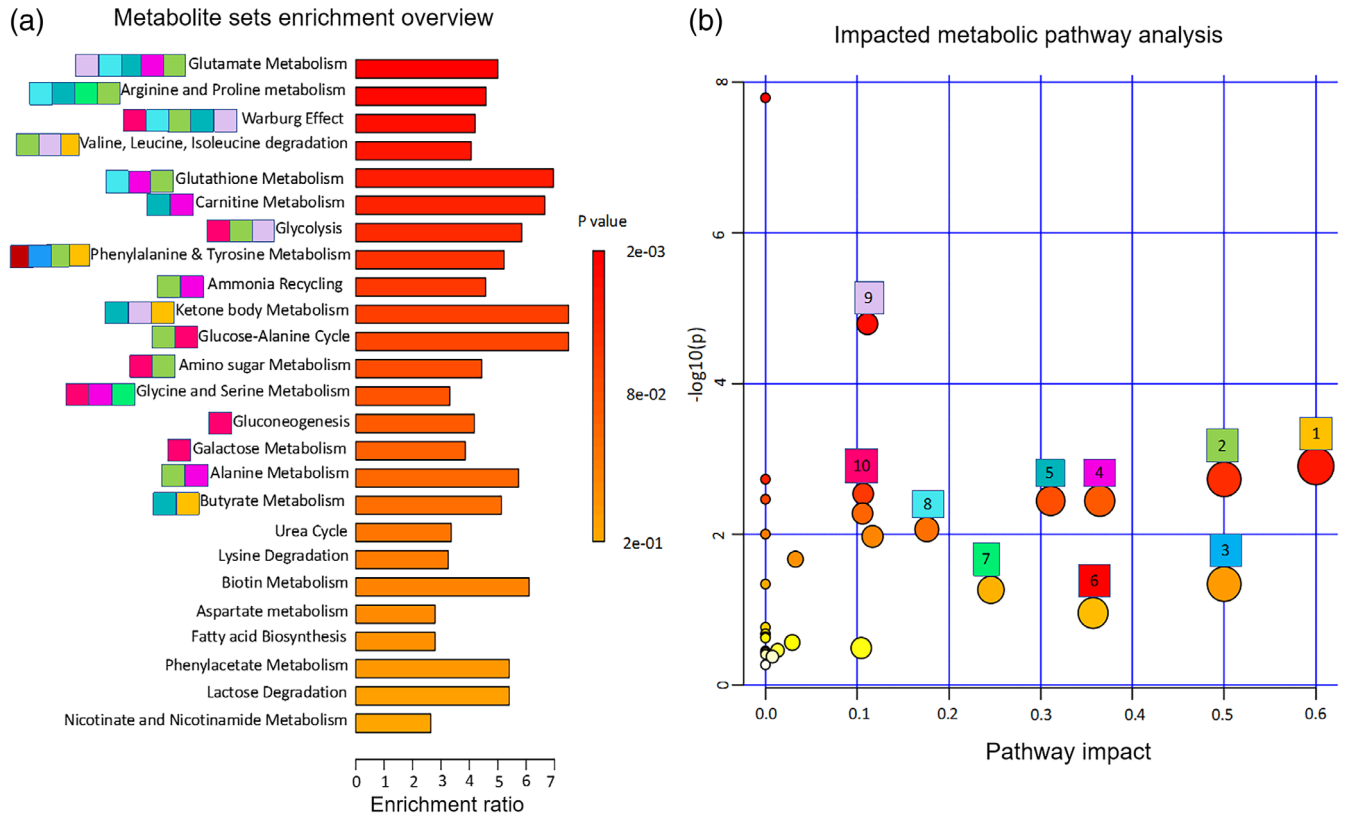

FIGURE 9 Plot summarizing metabolite set enrichment analysis (MSEA) and metabolic pathway impact analysis. (a) The MSEA was analyzed by using MetPA 5.0. through a one-column compound analysis. Fifteen metabolites are based on the VIP Score uploaded. The MSEA ranked based on the calculated *p*-value; the red color of the correlation plot indicated the smallest *p*-value. The small colored boxes of yellow, green, blue, pink, red, dark green, light pink, and purple correspond to the impacted metabolic pathway as suggested by the metabolic pathway impact view analysis. (b) Impacted metabolic pathway analysis. Each circle represents one metabolic pathway. Darker circle colors represent a smaller *p*-value, while the process size corresponds to the pathway impact score. The *y*-axis represents the *p*-value of Logl0, and the *x*-axis is metabolic impact. Thus, the larger circle size shows a more impact metabolic pathway by treating SARS-CoV-2 spike protein. Each circle is marked with numbers and colors for specific ways that are summarized. The impact score is more than 0.1; metabolic pathways are (1) synthesis and degradation of ketone bodies, (2) D-glutamine and D-glutamate metabolism, (3) phenylalanine, tyrosine, and tryptophan biosynthesis, (4) glutathione metabolism, (5) alanine, aspartate, and glutamate metabolism, (6) phenylalanine metabolism, (7) glycine, serine and threonine metabolism, (8) arginine and proline metabolism, (9) butanoate metabolism, and (10) glycolysis/gluconeogenesis. The data are reported as mean ± SD of three independent experiments

treating SARS-CoV-2 spike protein in PMA-induced THP-1 cells. These metabolites involved glycine, serine, and threonine metabolism, affecting the metabolic pathway. Generally, both ethanolamine and glycine are generated from serine via acetyl-CoA, which is part of the glycolysis and TCA cycle (Locasale, 2013; Shi & Tu, 2015). Acetyl-CoA could be generated from oxidative decarboxylation of pyruvate from the glycolysis (Shi & Tu, 2015). However, pyruvate was not detected in the SARS-CoV-2 spike-protein group cells. It implies that acetyl-CoA could be synthesized from another metabolic pathway. Therefore, phenylalanine and acetoacetate were detected in the spike protein-treated cells, which are comparatively less than the control. It was involved in phenylalanine metabolism. Acetoacetate is a ketone body generated from the phenylalanine metabolism (Kaufman, 1999). This acetoacetate can be converted into acetyl-CoA in the presence of the enzyme β-ketoacyl-CoA transferase (Dhillon & Gupta, 2022). It suggests why glycine, ethanolamine, sarcosine, and GPC were significantly reduced upon treating the spike protein in PMA-induced THP-1 cells and altered metabolomic profile.

Metabolomic corrections are a new approach that functionally and chemically against metabolomic-related diseases (Miranda-Massari et al., 2016) based on ^{1}H-NMR. Thus, we have investigated the effect of the natural compounds knowns as antcin A from fruiting bodies of *T. camphoratus* using the ^{1}H-NMR, which structurally resembles dexamethasone. It has the capability of an anti-inflammation (Chen et al., 2011). It was observed that phenylalanine, acetoacetate, and glucose increased dramatically by treatment of antcin A in the spike-protein treated group, directly enhancing the acetyl-CoA production, which produced a high amount of ethanolamine and correction of both phenylalanine and serine, glycine, and threonine metabolism. It implies that Antcin A is not restricted for anti-inflammation but is used to correct the metabolomic alteration mediated by SARS-CoV-2 spike protein.

10991573, 0, Downloaded from https://onlinelibrary.wiley.com/doi/10.1002/ptr.7670 by Natl Chung Hsing University, Wiley Online Library on [22/11/2022]. See the Terms and Conditions (https://onlinelibrary.wiley.com/terms-and-conditions) on Wiley Online Library for rules of use; OA articles are governed by the applicable Creative Commons License

PEP is more than just an energy-bonding chemical related to glycolysis. Increasing PEP elevates hydrogen peroxide (H_2O_2), which causes a reduction in the cell variability (Kondo et al., 2012) and observes reduced cell viability and increased PEP significantly upon spike protein treatment, but pyruvate was not detected. This indicates that spike protein increases PEP, which reduces cell viability since this PEP cannot convert into pyruvate. However, antcin A decreases the PEP production, which increases cell viability as antcin A did not show any cytotoxicity even at 50 μM for 48 h incubation. Glutamate is an essential metabolic link between the TCA and the urea cycles involved in cellular energy metabolism and the PEP production (Burrin & Stoll, 2009). We observed that both glutamine and glutamate increased significantly in the spike protein-treated groups, elevating α-KG synthesis and producing excessive succinate. It was reported that succinate covert into oxaloacetate via the TCA cycle (Martinez-Reyes & Chandel, 2020). The conversion of oxaloacetate into PEP is a possible reason that makes a high amount of PEP in the spike protein-treated groups that cannot be converted into pyruvate (Riedel et al., 2001).

In contrast, both glutamine and glutamate are reduced by the presence of the antcin A in spike-treated cells, which implies the reduction of PEP in the antcin A treated group. Besides, the presence of spike protein in the PMA-induced THP-1 cells produced more asparagine through alanine, glutamine, and aspartate metabolism. Thus, it interferes with $_D$-glutamate and glutamine, and glutamine and glutamate act as the primary precursor of metabolic changes. Moreover, it was corrected in the presence of antcin A but not dexamethasone (Figure 10).

SARS-CoV-2 spike protein enters the host cell via ACE2. It activates the TLR4 to induce inflammation that leads to progress and severity in the COVID-19 patient (Zhao et al., 2021), which may interfere with the metabolomic pathway. This study shows that 100 ng/mL of spike protein increases TLR4 and ACE2 expression significantly at the mRNA level, which may be the reason for the reduction in the cell viability and alteration of metabolomic profiles because we found that both dexamethasone and antcin A have not shown any cytotoxicity and reduced the expression the ACE2 and TLR4. However, only antcin-A rescued the metabolomic alteration, not dexamethasone. In addition, our previous study found that up to a dose of 10 mg/kg of antcin A did not cause observable physiological changes or mortality in mice (Kumar et al., 2019). Furthermore, the human equivalent dose (HED) of antcin A is 0.813 mg/kg, and the estimated human dose is

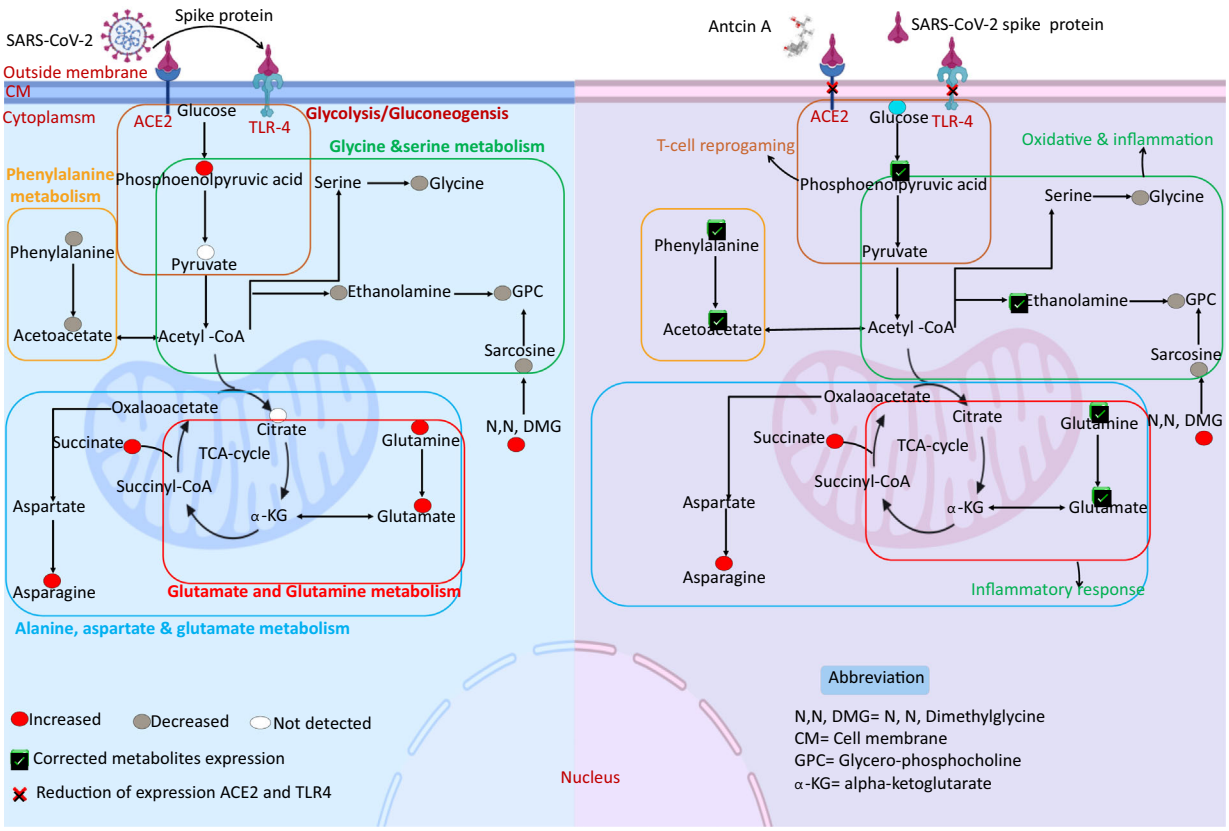

FIGURE 10 The schematic diagram illustrates alteration in the level of metabolites and the possible impacted metabolic pathway of the PMA-induced THP-1 cells for SARS-CoV-2 spike protein treated groups. The metabolites and metabolic pathways in light blue (left-hand side indicated the increased and reduced level of metabolites in the presence of SARS-CoV-2 spike protein in the PMA-induced THP-1 cells (macrophage-like cells) compared to the control group. Meanwhile, the purple-shaded color in the right-hand side indicated metabolic correction or reversing action of the SARS-CoV-2 spike in the presence of the antcin A from *T. camphoratus*. It also showed that the metabolic alteration meditated by the SARS-CoV-2 spike protein is highly relevant to inflammation

10991573, 0, Downloaded from https://onlinelibrary.wiley.com/doi/10.1002/ptr.7670 by Natl Chung Hsing University, Wiley Online Library on [22/11/2022]. See the Terms and Conditions (https://onlinelibrary.wiley.com/terms-and-conditions) on Wiley Online Library for rules of use; OA articles are governed by the applicable Creative Commons License

56.9 mg. The metabolomic alteration mediated by SARS-CoV-2 spike protein in THP-1 cells may not occur via activation of the receptors like TLR4 and ACE2 (Figure 10).

5 | CONCLUSION

Antcin A has similar structural properties to dexamethasone, which is used to treat COVID-19 patients due to its antiinflammatory properties. This study found that treatment with antcin A remarkably modulates SARS-CoV-2 spike protein-induced metabolomic alterations in PMA-induced THP-1 cells using a ^{1}H-NMR-based metabolomic approach. It presents a significant analytical challenge because it measures molecules with disparate physical properties, unlike genomic and proteomic methods. This study also revealed that antcin A treatment significantly blocked SARS-CoV-2 spike protein-induced up-regulation of TLR-4 and ACE2 receptors, critical factors of SARS-CoV-2 infection-mediated inflammation. Metabolite alteration is mediated by SARS-CoV-2 spike protein, not directly through activation of the spike receptors such as TLR4 and ACE2, which induce metabolomic alteration. These results clearly explain that SARS-CoV-2 spike protein alters metabolic pathways that are not associated with causing inflammation-associated signaling pathways in macrophage cells, which can be blocked by antcin A. Therefore, antcin A could be considered to develop functional medicine and drug therapies for viral infections related to metabolomic abnormalities.

CONFLICT OF INTEREST

The authors declare that there is no conflict of interest.

DATA AVAILABILITY STATEMENT

The data supporting this study's findings are available in this article's supplementary materials.

ORCID

Kanthasamy Jayabal Senthil Kumar https://orcid.org/0000-0002-8310-0546

Sheng-Yang Wang https://orcid.org/0000-0002-8579-3569

REFERENCES

Abdul-Hamid, N. A., Abas, F., Ismail, I. S., Tham, C. L., Maulidiani, M., Mediani, A., … Umashankar, S. (2019). ^{1}H-NMR-based metabolomics to investigate the effects of *Phoenix dactylifera* seed extracts in LPS-IFN-gamma-induced RAW 264.7 cells. *Food Research International*, *125*, 108565. https://doi.org/10.1016/j.foodres.2019.108565

Anderson, N. M., Mucka, P., Kern, J. G., & Feng, H. (2018). The emerging role and targetability of the TCA cycle in cancer metabolism. *Protein & Cell*, *9*(2), 216–237. https://doi.org/10.1007/s13238-017-0451-1

Burrin, D. G., & Stoll, B. (2009). Metabolic fate and function of dietary glutamate in the gut. *The American Journal of Clinical Nutrition*, *90*(3), 850 S–856 S. https://doi.org/10.3945/ajcn.2009.27462Y

Carlos, A. J., Ha, D. P., Yeh, D. W., Van Krieken, R., Tseng, C. C., Zhang, P., … Lee, A. S. (2021). The chaperone GRP78 is a host auxiliary factor for SARS-CoV-2 and GRP78 depleting antibody blocks viral entry and infection. *Journal of Biological Chemistry*, *296*, ARTN 100759. https://doi.org/10.1016/j.jbc.2021.100759

Cengiz, M., Borku Uysal, B., Ikitimur, H., Ozcan, E., Islamoglu, M. S., Aktepe, E., … Yavuzer, S. (2020). Effect of oral l-glutamine supplementation on Covid-19 treatment. *Clin Nutr Exp*, *33*, 24–31. https://doi.org/10.1016/j.yclnex.2020.07.003

Chen, Y. C., Liu, Y. L., Li, F. Y., Chang, C. I., Wang, S. Y., Lee, K. Y., … Tzen, J. T. (2011). Antcin a, a steroid-like compound from *Antrodia camphorata*, exerts anti-inflammatory effect via mimicking glucocorticoids. *Acta Pharmacologica Sinica*, *32*(7), 904–911. https://doi.org/10.1038/aps.2011.36

Chong, J., Wishart, D. S., & Xia, J. (2019). Using metaboanalyst 4.0 for comprehensive and integrative metabolomics data analysis. *Current Protocols in Bioinformatics*, *68*(1), e86. https://doi.org/10.1002/cpbi.86

Dhillon, K. K., & Gupta, S. (2022). *Biochemistry, ketogenesis*. Treasure Island (FL): StatPearls.

Dietmair, S., Timmins, N. E., Gray, P. P., Nielsen, L. K., & Kromer, J. O. (2010). Towards quantitative metabolomics of mammalian cells: Development of a metabolite extraction protocol. *Analytical Biochemistry*, *404*(2), 155–164. https://doi.org/10.1016/j.ab.2010.04.031

Feehan, J., & Apostolopoulos, V. (2021). Is COVID-19 the worst pandemic? *Maturitas*, *149*, 56–58. https://doi.org/10.1016/j.maturitas.2021.02.001

Geethangili, M., & Tzeng, Y. M. (2011). Review of pharmacological effects of *Antrodia camphorata* and its bioactive compounds. *Evidence-based Complementary and Alternative Medicine*, *2011*, 212641. https://doi.org/10.1093/ecam/nep108

Grimes, J. M., & Grimes, K. V. (2020). p38 MAPK inhibition: A promising therapeutic approach for COVID-19. *Journal of Molecular and Cellular Cardiology*, *144*, 63–65. https://doi.org/10.1016/j.yjmcc.2020.05.007

Group, R.C, Horby, P., Lim, W. S., Emberson, J. R., Mafham, M., Bell, J. L., … Landray, M. J. (2020). Dexamethasone in hospitalized patients with Covid-19 - preliminary report. *The New England Journal of Medicine*, *384*, 693–704. https://doi.org/10.1056/NEJMoa2021436

Han, J., Zhang, L., Guo, H., Wysham, W. Z., Roque, D. R., Willson, A. K., … Bae-Jump, V. L. (2015). Glucose promotes cell proliferation, glucose uptake and invasion in endometrial cancer cells via AMPK/mTOR/S6 and MAPK signaling. *Gynecologic Oncology*, *138*(3), 668–675. https://doi.org/10.1016/j.ygyno.2015.06.036

Hojyo, S., Uchida, M., Tanaka, K., Hasebe, R., Tanaka, Y., Murakami, M., & Hirano, T. (2020). How COVID-19 induces cytokine storm with high mortality. *Inflamm Regen*, *40*, 37. https://doi.org/10.1186/s41232-020-00146-3

Jacob, M., Lopata, A. L., Dasouki, M., & Abdel Rahman, A. M. (2019). Metabolomics toward personalized medicine. *Mass Spectrometry Reviews*, *38*(3), 221–238. https://doi.org/10.1002/mas.21548

Jalloh, I., Helmy, A., Howe, D. J., Shannon, R. J., Grice, P., Mason, A., … Carpenter, K. L. H. (2017). Focally perfused succinate potentiates brain metabolism in head injury patients. *Journal of Cerebral Blood Flow and Metabolism*, *37*(7), 2626–2638. https://doi.org/10.1177/0271678x16672665

Kaufman, S. (1999). A model of human phenylalanine metabolism in normal subjects and in phenylketonuric patients. *Proceedings of the National Academy of Sciences of the United States of America*, *96*(6), 3160–3164. https://doi.org/10.1073/pnas.96.6.3160

Kondo, Y., Ishitsuka, Y., Kadowaki, D., Kuroda, M., Tanaka, Y., Nagatome, M., … Irie, T. (2012). Phosphoenolpyruvic acid, an intermediary metabolite of glycolysis, as a potential cytoprotectant and antioxidant in heLa cells. *Biological & Pharmaceutical Bulletin*, *35*(4), 606–611. https://doi.org/10.1248/bpb.35.606

Kumar, K. J. S., Vani, M. G., Hsieh, H. W., Lin, C. C., Liao, J. W., Chueh, P. J., & Wang, S. Y. (2019). MicroRNA-708 activation by glucocorticoid receptor agonists regulate breast cancer tumorigenesis and metastasis via down-regulation of NF-κB signaling. *Carcinogenesis*, *40*(2), 335–348.

Kumar, K. J. S., Vani, M. G., Hsieh, H. W., Lin, C. C., & Wang, S. Y. (2021). Antcins from *Antrodia cinnamomea* and *Antrodia salmonea* inhibit angiotensin-converting enzyme 2 (ACE2) in epithelial cells: Can be potential candidates for the development of SARS-CoV-2 prophylactic

10991573, 0, Downloaded from https://onlinelibrary.wiley.com/doi/10.1002/ptr.7670 by Natl Chung Hsing University, Wiley Online Library on [22/11/2022]. See the Terms and Conditions (https://onlinelibrary.wiley.com/terms-and-conditions) on Wiley Online Library for rules of use; OA articles are governed by the applicable Creative Commons License

agents. *Plants-Basel*, *10*(8), ARTN 1736. https://doi.org/10.3390/plants10081736

Li, C. Y. (2020). Can glycine mitigate COVID-19 associated tissue damage and cytokine storm? *Radiation Research*, *194*(3), 199–201. https://doi.org/10.1667/RADE-20-00146.1

Locasale, J. W. (2013). Serine, glycine and one-carbon units: Cancer metabolism in full circle. *Nature Reviews. Cancer*, *13*(8), 572–583. https://doi.org/10.1038/nrc3557

Lu, R., Zhao, X., Li, J., Niu, P., Yang, B., Wu, H., … Tan, W. (2020). Genomic characterisation and epidemiology of 2019 novel coronavirus: Implications for virus origins and receptor binding. *Lancet*, *395*(10224), 565–574. https://doi.org/10.1016/S0140-6736(20)30251-8

Luo, X., Gu, X., & Li, L. (2018). Development of a simple and efficient method of harvesting and lysing adherent mammalian cells for chemical isotope labeling LC-MS-based cellular metabolomics. *Analytica Chimica Acta*, *1037*, 97–106. https://doi.org/10.1016/j.aca.2017.11.054

Malone, B., Urakova, N., Snijder, E. J., & Campbell, E. A. (2022). Structures and functions of coronavirus replication-transcription complexes and their relevance for SARS-CoV-2 drug design. *Nature Reviews. Molecular Cell Biology*, *23*(1), 21–39. https://doi.org/10.1038/s41580-021-00432-z

Martinez-Reyes, I., & Chandel, N. S. (2020). Mitochondrial TCA cycle metabolites control physiology and disease. *Nature Communications*, *11*(1), 102. https://doi.org/10.1038/s41467-019-13668-3

Merad, M., & Martin, J. C. (2020). Pathological inflammation in patients with COVID-19: A key role for monocytes and macrophages. *Nature Reviews. Immunology*, *20*(6), 355–362. https://doi.org/10.1038/s41577-020-0331-4

Miranda-Massari, J. R., Rodriguez-Gomez, J. R., Gonzalez, M. J., Cidre, C., Duconge, J., Marin, H., … McLeod, H. L. (2016). Metabolic correction in patients sample with diabetes: Clinical outcomes and costs reductions. *International Journal of Diabetes Research*, *5*(5), 92–101.

Nassar, A., Ibrahim, I. M., Amin, F. G., Magdy, M., Elgharib, A. M., Azzam, E. B., … Elfiky, A. A. (2021). A review of human coronaviruses' receptors: The host-cell targets for the crown bearing viruses. *Molecules*, *26*(21), 6455. https://doi.org/10.3390/molecules26216455

Richter, E., Ventz, K., Harms, M., & Hochgrafe, F. (2016). Induction of macrophage function in human THP-1 cells is associated with rewiring of MAPK signaling and activation of MAP3K7 (TAK1) protein kinase. *Frontiers in Cell and Development Biology*, *4*, ARTN 21. https://doi.org/10.3389/fcell.2016.00021

Riedel, C., Rittmann, D., Dangel, P., Mockel, B., Petersen, S., Sahm, H., & Eikmanns, B. J. (2001). Characterization of the phosphoenolpyruvate carboxykinase gene from Corynebacterium glutamicum and significance of the enzyme for growth and amino acid production. *Journal of Molecular Microbiology and Biotechnology*, *3*(4), 573–583.

Senthil Kumar, K. J., Gokila Vani, M., Chen, C. Y., Hsiao, W. W., Li, J., Lin, Z. X., … Wang, S. Y. (2020). A mechanistic and empirical review of antcins, a new class of phytosterols of formosan fungi origin. *Journal of Food and Drug Analysis*, *28*(1), 38–59. https://doi.org/10.1016/j.jfda.2019.09.001

Shang, J., Wan, Y., Luo, C., Ye, G., Geng, Q., Auerbach, A., & Li, F. (2020). Cell entry mechanisms of SARS-CoV-2. *Proceedings of the National Academy of Sciences of the United States of America*, *117*(21), 11727–11734. https://doi.org/10.1073/pnas.2003138117

Sharun, K., Tiwari, R., Dhama, J., & Dhama, K. (2020). Dexamethasone to combat cytokine storm in COVID-19: Clinical trials and preliminary evidence. *International Journal of Surgery*, *82*, 179–181. https://doi.org/10.1016/j.ijsu.2020.08.038

Shi, L., & Tu, B. P. (2015). Acetyl-CoA and the regulation of metabolism: Mechanisms and consequences. *Current Opinion in Cell Biology*, *33*, 125–131. https://doi.org/10.1016/j.ceb.2015.02.003

Thomas, T., Stefanoni, D., Reisz, J. A., Nemkov, T., Bertolone, L., Francis, R. O., … D'Alessandro, A. (2020). COVID-19 infection alters kynurenine and fatty acid metabolism, correlating with IL-6 levels and renal status. *JCI Insight*, *5*(14), e140327. https://doi.org/10.1172/jci.insight.140327

Valipour, M., Irannejad, H., & Emami, S. (2022a). Application of emetine in SARS-CoV-2 treatment: Regulation of p38 MAPK signaling pathway for preventing emetine-induced cardiac complications. *Cell Cycle*, *1–8*, 1–8. https://doi.org/10.1080/15384101.2022.2100575

Valipour, M., Irannejad, H., & Emami, S. (2022b). Papaverine, a promising therapeutic agent for the treatment of COVID-19 patients with underlying cardiovascular diseases (CVDs). *Drug Development Research*, *83*(6), 1246–1250. https://doi.org/10.1002/ddr.21961

Valipour, M., Zarghi, A., Ebrahimzadeh, M. A., & Irannejad, H. (2021). Therapeutic potential of chelerythrine as a multi-purpose adjuvant for the treatment of COVID-19. *Cell Cycle*, *20*(22), 2321–2336. https://doi.org/10.1080/15384101.2021.1982509

Wishart, D. S. (2019). Metabolomics for investigating physiological and pathophysiological processes. *Physiological Reviews*, *99*(4), 1819–1875. https://doi.org/10.1152/physrev.00035.2018

Wrapp, D., Wang, N., Corbett, K. S., Goldsmith, J. A., Hsieh, C. L., Abiona, O., … McLellan, J. S. (2020). Cryo-EM structure of the 2019-nCoV spike in the prefusion conformation. *Science*, *367*(6483), 1260–1263.

Wu, D., Shu, T., Yang, X., Song, J. X., Zhang, M., Yao, C., … Zhou, X. (2020). Plasma metabolomic and lipidomic alterations associated with COVID-19. *National Science Review*, *7*(7), 1157–1168. https://doi.org/10.1093/nsr/nwaa086

Zhao, Y., Kuang, M., Li, J., Zhu, L., Jia, Z., Guo, X., … You, F. (2021). SARS-CoV-2 spike protein interacts with and activates TLR41. *Cell Research*, *31*, 818–820. https://doi.org/10.1038/s41422-021-00495-9

SUPPORTING INFORMATION

Additional supporting information can be found online in the Supporting Information section at the end of this article.

How to cite this article: Dakpa, G., Senthil Kumar, K. J., Tsao, N.-W., & Wang, S.-Y. (2022). Antcin A, a phytosterol regulates SARS-CoV-2 spike protein-mediated metabolic alteration in THP-1 cells explored by the ^{1}H-NMR-based metabolomics approach. *Phytotherapy Research*, 1–18. https://doi.org/10.1002/ptr.7670

10991573, 0, Downloaded from https://onlinelibrary.wiley.com/doi/10.1002/ptr.7670 by Natl Chung Hsing University, Wiley Online Library on [22/11/2022]. See the Terms and Conditions (https://onlinelibrary.wiley.com/terms-and-conditions) on Wiley Online Library for rules of use; OA articles are governed by the applicable Creative Commons License